

AD \_\_\_\_\_

Award Number: DAMD17-97-1-7204

TITLE: Role of IGFBP-3/IGFBP-3 Receptor Interaction in Normal and Malignant Mammary Growth: A Potential Diagnostic Parameter and New Strategy for Endocrine Therapy

PRINCIPAL INVESTIGATOR: Youngman Oh, Ph.D.

CONTRACTING ORGANIZATION: Oregon Health Sciences University  
Portland, Oregon 97201-3098

REPORT DATE: September 2000

TYPE OF REPORT: Annual

PREPARED FOR: U.S. Army Medical Research and Materiel Command  
Fort Detrick, Maryland 21702-5012

DISTRIBUTION STATEMENT: Approved for Public Release;  
Distribution Unlimited

The views, opinions and/or findings contained in this report are those of the author(s) and should not be construed as an official Department of the Army position, policy or decision unless so designated by other documentation.

# REPORT DOCUMENTATION PAGE

OMB No. 074-0188

Public reporting burden for this collection of information is estimated to average 1 hour per response, including the time for reviewing instructions, searching existing data sources, gathering and maintaining the data needed, and completing and reviewing this collection of information. Send comments regarding this burden estimate or any other aspect of this collection of information, including suggestions for reducing this burden to Washington Headquarters Services, Directorate for Information Operations and Reports, 1215 Jefferson Davis Highway, Suite 1204, Arlington, VA 22202-4302, and to the Office of Management and Budget, Paperwork Reduction Project (0704-0188), Washington, DC 20503

1. AGENCY USE ONLY (Leave blank)	2. REPORT DATE	3. REPORT TYPE AND DATES COVERED	
	September 2000	Annual (1 Sep 99 - 31 Aug 00)	
4. TITLE AND SUBTITLE Role of IGFBP-3/IGFBP-3 Receptor Interaction in Normal and Malignant Mammary Growth: A Potential Diagnostic Parameter and New Strategy for Endocrine Therapy		5. FUNDING NUMBERS DAMD17-97-1-7204	
6. AUTHOR(S) Youngman Oh, Ph.D.			
7. PERFORMING ORGANIZATION NAME(S) AND ADDRESS(ES) Oregon Health Sciences University Portland, Oregon 97201-3098		8. PERFORMING ORGANIZATION REPORT NUMBER	
E-MAIL: ohy@ohsu.edu			
9. SPONSORING / MONITORING AGENCY NAME(S) AND ADDRESS(ES) U.S. Army Medical Research and Materiel Command Fort Detrick, Maryland 21702-5012		10. SPONSORING / MONITORING AGENCY REPORT NUMBER	
11. SUPPLEMENTARY NOTES			
12a. DISTRIBUTION / AVAILABILITY STATEMENT Approved for public release; distribution unlimited			12b. DISTRIBUTION CODE
13. ABSTRACT: The proposal of my grant is to investigate the biological significance and mechanism of insulin-like growth factor binding protein-3 (IGFBP-3) as well as identification and characterization of the IGFBP-3 receptor in human breast cancer cells. As a third year task, we have successfully characterized binding specificity of the IGFBP-3 receptor to IGFBP-3. It revealed that only IGFBP-3 and its fragment (aa88-148) bind the IGFBP-3 receptor with high affinity, whereas IGFBPs, -2, 4-, -5 and -6 did not interact with the IGFBP-3 receptor, demonstrating specificity of the IGFBP-3 receptor. We have also identified the IGFBP-3/IGFBP-3 receptor-mediated signal transduction pathway in human breast cancer cells. Current studies demonstrated that the IGFBP-3/IGFBP-3 receptor axis causes cell cycle arrest in G1 phase and induces apoptosis. The underlying mechanisms are ablation of MAPK signaling cascades and increase of caspase activity, respectively. Further through investigation is currently in the process in my laboratory. As characterization of the structure-functional analysis of IGFBP-3 and the IGFBP-3 receptor, we identified differential effects of IGFBP-3 and those IGFBP-3 proteolytic fragments on ligand binding, cell surface association and IGF-I receptor signaling. Current findings under this grant support will provide pivotal evidence for clinical significance and potential application of the IGFBP-3/IGFBP-3 receptor axis in the prevention and/or treatment of human neoplasia, in particular, breast cancer.			
14. SUBJECT TERMS Breast Cancer			15. NUMBER OF PAGES 47
			16. PRICE CODE
17. SECURITY CLASSIFICATION OF REPORT Unclassified	18. SECURITY CLASSIFICATION OF THIS PAGE Unclassified	19. SECURITY CLASSIFICATION OF ABSTRACT Unclassified	20. LIMITATION OF ABSTRACT Unlimited

NSN 7540-01-280-5500

Standard Form 298 (Rev. 2-89)  
Prescribed by ANSI Std. Z39-18  
298-102

## **TABLE OF CONTENTS**

<b>Front Cover</b>	<b>1</b>
<b>Report Documentation Page</b>	<b>2</b>
<b>Table of Contents</b>	<b>3</b>
<b>Introduction</b>	<b>4</b>
<b>Body</b>	<b>4</b>
<b>Key Research Accomplishments</b>	<b>11</b>
<b>Reportable Outcomes</b>	<b>12</b>
<b>Conclusions</b>	<b>12</b>
<b>Appendices</b>	<b>13</b>

## I. INTRODUCTION.

The insulin-like growth factor binding proteins (IGFBPs) 1-6 bind IGF-I and IGF-II with high affinity and serve to transport the IGFs, prolong their half-lives, and modulate their proliferative and anabolic effects on target cells. The molecular mechanisms involved in the interaction of the IGFBPs with the IGFs and their receptors remain unclear, but these molecules appear, at least, to regulate the availability of free IGFs for interaction with IGF receptors. Recent studies from our laboratory and others demonstrated that some IGFBPs have ability to exert IGF-independent actions.

In this project, I proposed investigation of **the characterization of the IGFBP-3-specific receptor, the elucidation of the pertinent signal transduction pathways and analysis of structure-function relationships in the IGFBP-3** in the context of growth control in human breast cancer.

## II. BODY.

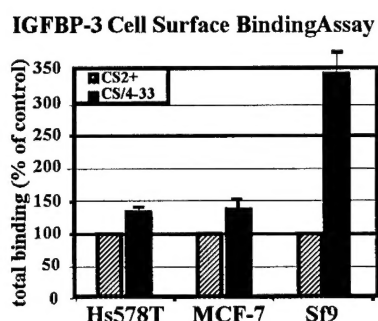
### I. characterization of the IGFBP-3 receptor in human breast cancer cells (Tasks 1-7).

In our continuing investigation of the biological importance of IGFBP-3, we are characterizing specificity of the IGFBP-3 receptor binding to IGFBP-3 and involvement of the IGFBP-3 receptor on the IGFBP-3-induced growth inhibition.

As IGFBP-3 has been previously reported to specifically bind to the surface of breast cancer cells and subsequently exhibit growth suppressing activity, I further determined whether the IGFBP-3 receptor might participate in this process. Hs578T and MCF-7 human breast cancer cells were transiently transfected with a construct encoding IGFBP-3 receptor FLAG-tagged at the C-terminus (4-33<sup>F</sup>) or with vector alone. These cells were then subjected to a monolayer binding assay using <sup>125</sup>I-labelled IGFBP-3. The overexpression of 4-33 resulted in a 30-60% increase in IGFBP-3 binding to the cell surface relative to cells expressing endogenous levels of 4-33 (Figure 1). This result was greatly magnified when the same assay was done using Sf9 insect cells either uninfected or infected with virus harboring the 4-33<sup>F</sup> cDNA, as the infected cells overexpress 4-33<sup>F</sup> to a much greater degree compared to control cells. In these cells the increase in IGFBP-3 cell surface binding was nearly 3.5 fold over control. The increased IGFBP-3 binding was competed in a dose-dependent manner with the addition of cold IGFBP-3, and was unaffected by the presence of the FLAG-tag at the C-terminus of the 4-33 protein. Further, fragments of IGFBP-3 containing the putative binding region for 4-33 (amino acids 88-148) were able to successfully compete labelled full-length IGFBP-3 binding, but an N-terminal fragment comprised

of amino acids 1-97 was not. Additionally, other IGF binding proteins were unable to compete IGFBP-3 binding in this assay, demonstrating IGFBP-3 specificity.

**A)**



**B)**

**Competitive Binding Results**

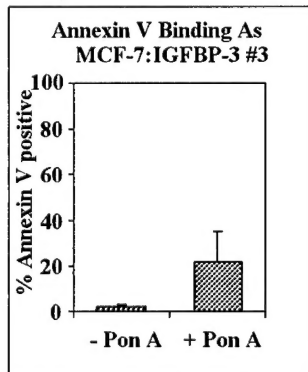
IGFBP-3 fragments:	IGFBP-3 <sup>(1-87)</sup>	-
IGFBP-3 <sup>(88-148)</sup>	+	
IGFBP-3 <sup>(88-264)</sup>	+	
Other binding proteins:		
IGFBP-2	-	
IGFBP-4	-	
IGFBP-5	-	
IGFBP-6	-	

**Figure 1.** A) Increased cell surface binding of IGFBP-3 to cells overexpressing 4-33. B) Competitive inhibition of IGFBP-3 cell surface binding with unlabelled IGFBP-3. Only fragments containing amino acids 88-148 were able to successfully compete full-length IGFBP-3 binding. Other IGF binding proteins were unable to compete.

### The IGFBP-3 receptor involvement in IGFBP-3 biological function: cell cycle arrest and apoptosis.

To facilitate the study of the biological actions of 4-33 and IGFBP-3, we have generated a stably-transfected inducible IGFBP-3 MCF-7 breast cancer cell line using the ecdysone-inducible system (see Appendix 1). One of the sublines, designated MCF-7:BP-3 #3 (colony #3), inducibly produced IGFBP-3 at levels comparable to the endogenous levels produced by Hs578T cells. The induction of IGFBP-3 in these cells caused inhibition of growth and DNA synthesis as measured by incorporation of [<sup>3</sup>H]thymidine, to a similar degree as has been described for treatment of MCF-7 cells with exogenous IGFBP-3. Induced expression of IGFBP-3 in these cells further leads to cell cycle arrest at G<sub>1</sub>. We observed an increase in the percentage of cell in G<sub>1</sub> from 72.1% to 78.1%, with a concurrent decrease in cells in S and G<sub>2</sub>/M phases (data not shown, see Appendix 1). Further, our data indicate that IGFBP-3 induces apoptosis in this cell system (Figure 2).

**A)**



**B)**

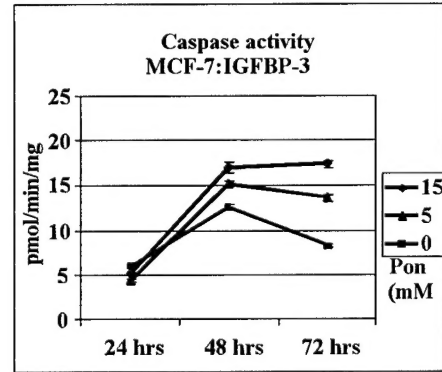
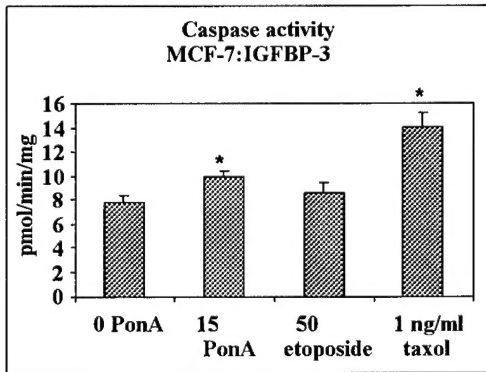


**Figure 2.** A) IGFBP-3-induced cell cycle arrest. B) IGFBP-3 induction of apoptosis, as measured by Annexin V binding and assays for caspase activity. \* = p<0.05.

Studies of 4-33 in breast cancer cells which produce IGFBP-3 demonstrated that transient overexpression of 4-33 resulted in a significant increase in cell detachment / death over time, compared to little or no effect in cells which do not produce IGFBP-3 (data not shown). IGFBP-3-expressing Hs578T cells displayed fewer cells per field following transient overexpression of 4-33 compared to transfection with vector alone, while no such effect was seen in IGFBP-3-nonexpressing MCF-7 cells. We further investigated the effect of 4-33 and IGFBP-3 on cell proliferation as indicated by incorporation of [<sup>3</sup>H]thymidine during DNA synthesis. We compared wild type MCF-7 cells with the MCF-7:BP-3 #3 subline, with and without incubation with ponasterone A. As expected, induction of IGFBP-3 by ponasterone A resulted in an inhibition of DNA synthesis to an average of 55% of control levels (Figure 3). With the additional overexpression of 4-33 in these cells, DNA synthesis was further inhibited down to an average of 35% of control levels. Overexpression of 4-33 had no significant effect on DNA

synthesis in the absence of IGFBP-3 (either wild type MCF-7 or uninduced MCF-7:BP-3 #3 cells), and ponasterone A had no inhibitory effect in wild type MCF-7 cells.

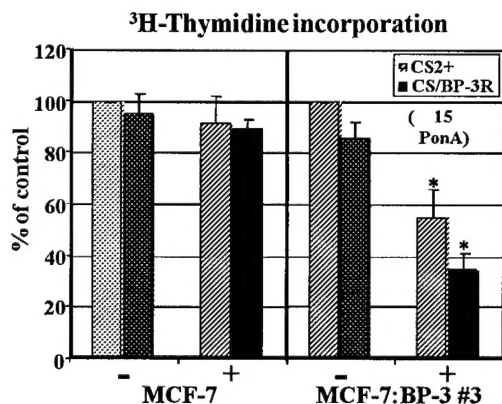


**Figure 3.** Growth inhibition of breast cancer cells by IGFBP-3 and 4-33. 4-33 enhances the IGFBP-3 growth-inhibitory effect on breast cancer cells as measured by thymidine incorporation. \* = p<0.05.

## 2. Identification of the IGFBP-3/IGFBP-3 receptor-induced signal transduction pathway (Tasks 8 and 9)

As reported last year, we have successfully generated inducible IGFBP-3 stably transfected human breast cancer cell line, MCF-7:IGFBP-3 #3 (see Appendix 1). Dose-dependent inducible production of IGFBP-3 protein was detected in the induced stably-transfected cells, compared to undetectable levels in control parental and uninduced stably-transfected cells. Induction of IGFBP-3 in these cells showed dose-dependent inhibition of DNA synthesis as assessed by [<sup>3</sup>H]-thymidine incorporation assays. This inhibitory effect was abolished by co-treatment with Y60L-

IGF-I, an IGF analog which has significantly reduced affinity for the IGF receptor but retains high affinity for IGFBP-3, demonstrating specificity and IGF-independence. In addition, flow cytometry analysis showed that induced expression of IGFBP-3 led to an arrest of the cell cycle in G1-S phase. Induction of IGFBP-3 resulted in a significant decrease in the mRNA and protein levels of cyclin D, but not cyclin E, as well as concomitant decreases in the levels of cdk4, total-Rb, and phosphorylated-Rb, consistent with and presenting a possible mechanism for IGFBP-3-induced cell cycle arrest. Moreover, IGFBP-3 inhibited oncogenic Ras-induced phosphorylation of MAPKs, presenting the evidence for cross-talk of IGFBP-3 signaling with MAPK signal transduction pathway. IGFBP-3-expressing cells also displayed increased Annexin V binding compared to controls, exhibiting the IGFBP-3-induced apoptosis. Further studies demonstrated that IGFBP-3 caused an increase in caspase activities, suggesting a potential mechanism for the IGFBP-3-induced apoptosis. Taken together, present study shows that cellular production of IGFBP-3 leads to cell cycle arrest and induction of apoptosis, thereby inhibiting cell proliferation in these MCF-7 human breast cancer cells and suggesting that IGFBP-3 functions as a negative regulator of breast cancer cell growth, independent of the IGF axis.

**Cell cycle arrest.** I examined the effect of the IGFBP-3 receptor on these specific proteins known to be involved in cell cycle progression and the apoptotic process. Hs578T and MCF-7 cells, and the IGFBP-3-constitutively expressing MCF-7:BP-3 #1 cell line were either left untreated, treated with an apoptosis inducer (sodium butyrate, NaB), or transfected with vector alone or the IGFBP-3 receptor. At 24 hours post-transfection cell lysates were harvested, assayed for protein content, and equal amounts of protein per sample were immunoblotted. Examination of cell cycle proteins cyclin D1, cyclin E, and p21/Waf1 revealed a specific decrease in the level of cyclin D1 protein in the IGFBP-3 receptor-transfected cells in the presence of IGFBP-3. Control transfected cells, and the IGFBP-3 receptor-transfected cells in the absence of IGFBP-3 had no effect on cyclin D1 levels. Cyclin E and p21/Waf1 were unaffected by these treatments, while proper induction of p21/Waf1 was seen with NaB treatment. Additionally, when the IGFBP-3 receptor-transfected cells were examined by immunofluorescence with antibodies against Cyclin D1, Rb and the IGFBP-3 receptor, a significant reduction in both Cyclin D1 and Rb immunodetectable protein levels occurred in 4-33-transfected cells, but not in neighboring untransfected cells (Figure 4).

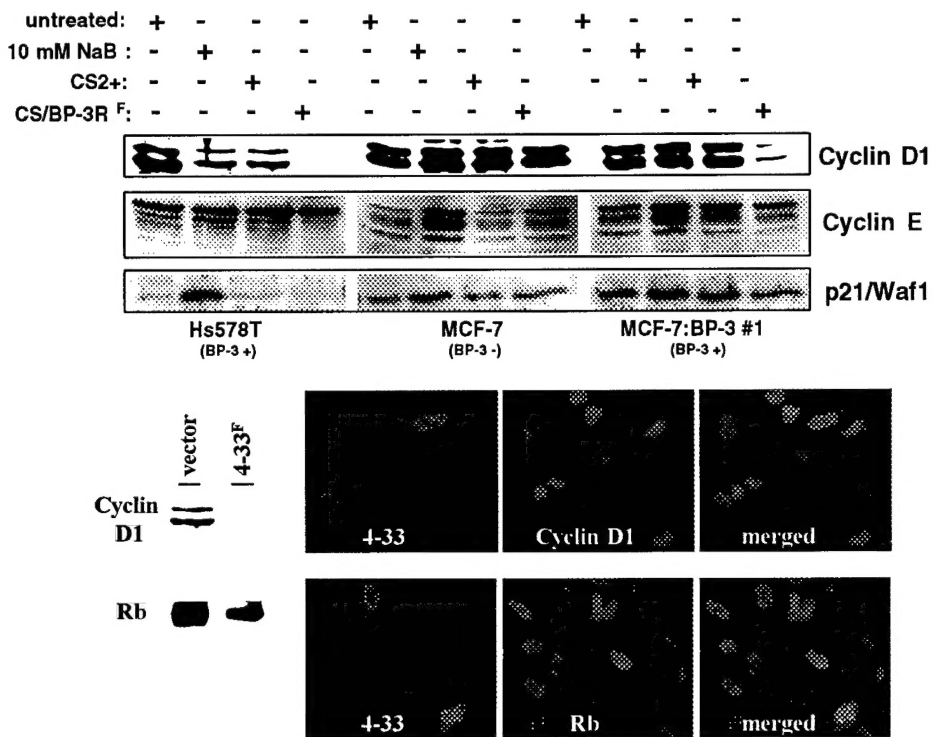


**Figure 4.** Effect of the IGFBP-3 receptor (4-33) and IGFBP-3 overexpression on cell cycle proteins in breast cancer cells. A) Specific decrease in the

level of Cyclin D1 in cells overexpressing 4-33. The levels of Cyclin E and p21/Waf1 were unaffected. B) Immunofluorescence data showing specific reduction of immunodetectable levels of Cyclin D1 and Rb proteins in cells overexpressing 4-33, but not in neighboring untransfected cells.

A possible mechanism for this effect may be perturbation of p44/42 mitogen-activated protein kinase (MAPK) signaling pathways. Our data indicate that levels of phosphorylated MAPK, Cyclin D1, and phosphorylated retinoblastoma (Rb) proteins are significantly reduced upon induction of IGFBP-3 expression in MCF-7:BP-3 #3 cells (Figure 5).

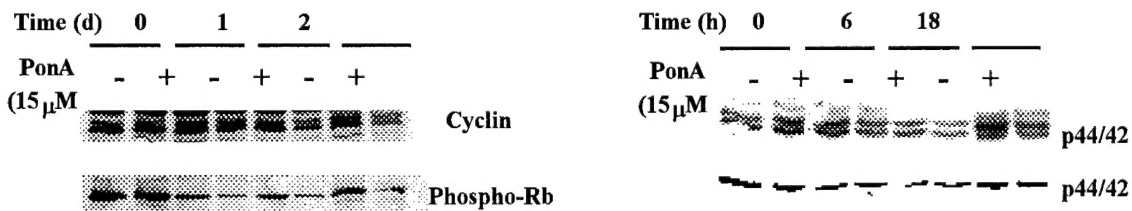


**Figure 5.** Western immunoblot and immunofluorescence data showing a significant decrease in the levels of phospho-p44/42 MAPK, Cyclin D1, and phospho-Rb proteins with induction of IGFBP-3 expression.

**Apoptosis:** We further investigated whether the IGFBP-3 receptor plays a role in IGFBP-3-induced apoptosis. Hs578T, MCF-7, and induced MCF-7:BP-3 #3 cells were either untreated or transfected with vector or 4-33 and the cell cycle profile was analyzed by propidium iodide staining of DNA content followed by flow cytometry detection (Figure 6A). In each case, the IGFBP-3 receptor-transfected cells displayed an increase in the sub-G1 population and a concurrent decrease in the S/G2/M population compared to control cells. A peak in the sub-G1 range can be indicative of cells undergoing apoptosis. We investigated this further using an Annexin V assay, which is used to identify cells early in the apoptotic process. By incubating suspended cells with FITC-labelled Annexin V, coupled with concurrent propidium iodide staining without permeabilization of the plasma membrane, it is possible to discriminate between cells in early apoptosis and those in late apoptosis or necrosis using a two-color flow cytometric analysis. Hs578T cells were transfected with vector alone or the IGFBP-3 receptor, and subsequently harvested and assayed at 14, 24, 36, and 48 hours post-transfection. As shown in Figure 6B, at each time point, the population of early apoptotic cells was significantly increased in the cells transfected with the IGFBP-3 receptor, compared to control-transfected cells.

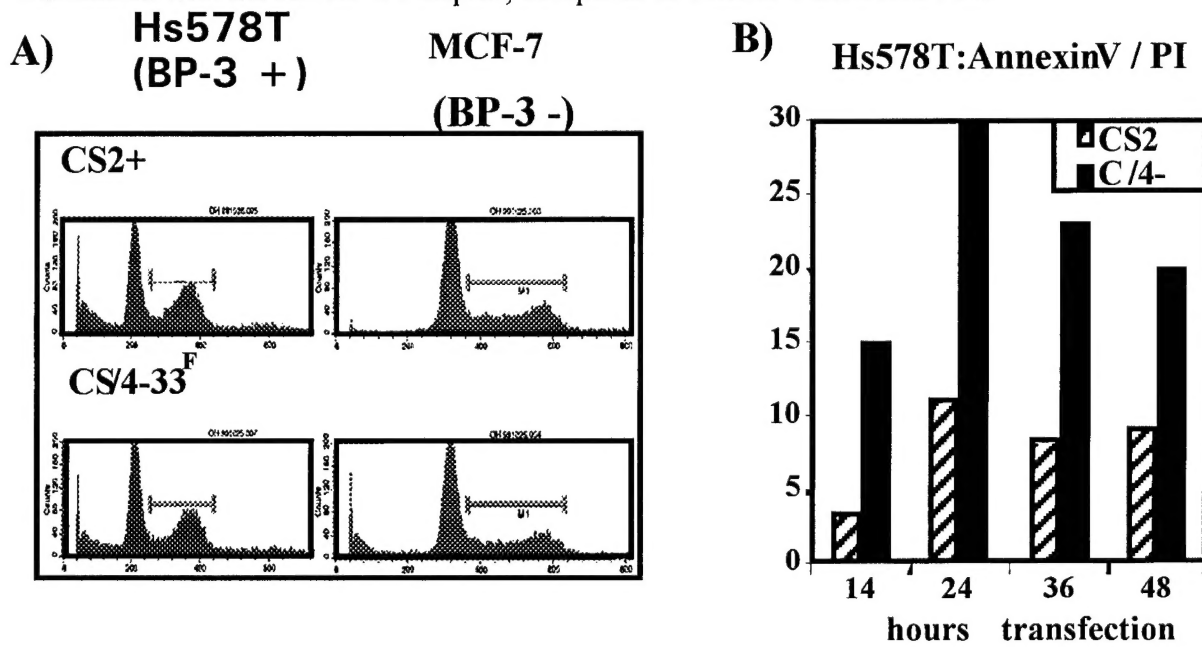


**Figure 6.** Induction of apoptosis by IGFBP-3 and the IGFBP-3 receptor (4-33). A) Cell cycle analysis of breast cancer cells either untransfected or transfected with vector or 4-33. B) Annexin V binding assay data from a time course of Hs578T cells transfected with vector or 4-33. Annexin V binding is an indicator of the early stages of apoptosis.

As IGFBP-3 has been shown to potentiate caspase activity, we examined this phenomenon as a potential mechanism for IGFBP-3/IGFBP-3 receptor biological function. Caspases are a family of evolutionarily related cysteine-dependent proteases, with a universal specificity for Asp in the P<sub>1</sub> position, that play a prominent role during the progression of apoptosis. Activation of caspases and subsequent cleavage of critical cellular substrates are implicated in many of the morphological and biochemical changes associated with apoptotic cell death. Using an assay which detects activity of a broad range of caspases by incubating cell lysates with a mixture of purified fluorogenic peptide caspase substrates and measuring subsequent reaction kinetics, we demonstrated a measurable and reproducible increase in caspase activity (described as pmol substrate cleaved / min / mg protein) in Hs578T cells with transient overexpression of 4-33 compared to control-transfected cells (Figure 7).

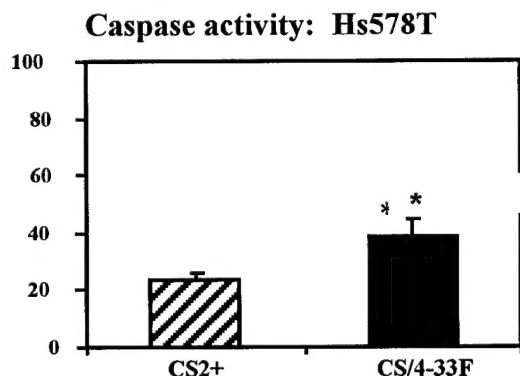


**Figure 7.** Potentiation of caspase activity in Hs578T cells transiently transfected with 4-33F compared to controls. \* = p<0.05.

### 3. Characterization of structure-function aspects of IGFBP-3 action in human breast cancer. (Tasks 10-13)

Our previous report demonstrated that we have generated proteolytic fragments derived from plasmin-digested recombinant human IGFBP-3, synthetic fragments generated using the baculovirus expression system, and IGFBP-3 fragments in normal human urine. With each of these reagents we demonstrated retention of IGF binding of an N-terminal IGFBP-3 fragment, albeit with significantly reduced affinity as compared to the intact molecule. In addition, we demonstrated that these N-terminal fragments can bind specifically to insulin, and inhibit insulin receptor autophosphorylation. As further investigation, we identified differential effects of IGFBP-3 and those IGFBP-3 proteolytic fragments on ligand binding, cell surface association and

IGF-I receptor signaling (see Appendix #2). We demonstrated that IGFBP-3 showed a dose-dependent inhibition of autophosphorylation of the beta-subunit of IGF-I receptor (IGFIR). The (1-97)NH<sub>2</sub>-terminal fragment inhibited IGFIR autophosphorylation at high concentrations and this effect appears largely due to sequestration of IGF-I. In contrast, no inhibition of IGF-I induced IGFIR autophosphorylation was detectable with the (98-264) and (184-264)COOH-terminal fragments, despite their ability to bind IGF. However, unlike the (1-97)NH<sub>2</sub>-terminal fragment, the COOH-terminal fragments of IGFBP-3 retained their ability to associate with the cell surface and this binding was competed by heparin, similar to intact IGFBP-3 (Appendix #2). In addition, we are in the progress to synthesize IGFBP-3 mutants which show no binding affinity to IGFs, but retain full affinity for the IGFBP-3 receptor.

These preliminary data support the hypothesis that 4-33 is a functional receptor for IGFBP-3 in the breast cancer system, and that the interaction of IGFBP-3 with 4-33 may be an important mechanism in the IGF-independent, growth-inhibitory actions of IGFBP-3. These studies firstly demonstrated the underlying mechanism for the IGF/IGFBP-3 receptor-induced biological function; the IGFBP-3/IGFBP-3 receptor axis arrests cell cycle progression through ablation of the MAPK signaling cascades, and induces apoptosis via potentiating caspase activities.

Current findings under this grant support will provide pivotal evidence for clinical significance and potential application of the IGFBP-3/IGFBP-3 receptor axis in the prevention and/or treatment of human neoplasia, in particular, breast cancer.

### **III. KEY RESEARCH ACCOMPLISHMENTS**

- Demonstration of the binding specificity of the IGFBP-3 receptor (4-33) to IGFBP-3 and other binding proteins.
- Characterization of the IGFBP-3-induced biological function in human breast cancer cells.
- Identification of the potential mechanisms for the IGFBP-3/IGFBP-3 receptor-mediated cell cycle arrest and induction of apoptosis.
- Characterization of IGFBP-3 proteolytic fragments on ligand binding, cell surface association and IGF-I receptor signaling.

#### **IV. REPORTABLE OUTCOMES**

- Devi, GR, et al., 2000. Endocrinology, in press.
- Kim, H-S, et al., 2000. J. Biol. Chem, in submission.
- Ingermann, A.R. and Oh, Y. 2000. 4<sup>th</sup> International Workhop on IGF Binding Proteins, Sydney, Australia.
- Kim, H-S and Oh, Y. 2000. 4<sup>th</sup> International Workhop on IGF Binding Proteins, Sydney, Australia.

#### **V. CONCLUSIONS:**

In summary, my laboratory has demonstrated IGFBP-3 / IGFBP-3 receptor interactions in the human breast cancer cell system, identified and initially characterized an IGFBP-3 interacting protein from breast cancer cells, and generated a polyclonal antibody against this interacting protein, and generated inducible IGFBP-3 stably transfected cell lines. Now, we have successfully characterized binding specificity of the IGFBP-3 receptor to IGFBP-3; Only IGFBP-3 and its fragment (aa88-148) bind the IGFBP-3 receptor with high affinity, whereas IGFBPs, -2, 4-, -5 and -6 did not interact with the IGFBP-3 receptor, demonstrating specificity of the IGFBP-3 receptor. We have also identified the IGFBP-3/IGFBP-3 receptor-mediated signal transduction pathway in human breast cancer cells. Current studies demonstrated that the IGFBP-3/IGFBP-3 receptor axis causes cell cycle arrest in G1 phase and induces apoptosis. The underlying mechanisms are ablation of MAPK signaling cascades and increase of caspase activity, respectively. Further through investigation is currently in the process in my laboratory. As characterization of the structure-functional analysis of IGFBP-3 and the IGFBP-3 receptor, we demonstrated that these N-terminal fragments can bind specifically to insulin, and inhibit insulin receptor autophosphorylation. As further investigation, we identified differential effects of IGFBP-3 and those IGFBP-3 proteolytic fragments on ligand binding, cell surface association and IGF-I receptor signaling. As laid out in the Statement of Work, We have completed Technical Objective 1, Tasks 1-7 in this year. We have accomplished Technical Objective 2, Tasks 8-9 and published 2 papers. Technical Objective 3, Tasks 10-11 are finished and published work. Tasks 11-12 are currently underway. In order to finish those Tasks, one-year extension was requested and proved by the U.S. Army Medical Research Committee

## **VI. APPENDICES**

1. Devi, GR, Yang, D-H, Rosenfeld, RG, Oh Y. Differential effects of insulin-like growth factor (IGF)-binding protein-3 and its proteolytic fragments on ligand binding, cell surface association, and IGF-I receptor signaling. *Endocrinology*, 2000, in press.
2. Kim, H-S, Ingermann AR, Tsubaki, J, Twigg, SM, Oh Y. Cellular expression of insulin-like growth factor binding protein-3 arrests the cell cycle and induces apoptosis in MCF-7 human breast cancer cells,. *J. Biol. Chem.*, 2000, in submission.

JOPNAME: END (ee) PAGE: 1 SESS: 2 OUTPUT: Thu Aug 24 06:01:14 2000  
 /ball8/ee-end/ee\_end/ee1100/cc7781 03a

SEARCHED:
Searched query
PAGE 1-4 24

0013-7227(00)60:2;0;0  
*Endocrinology*  
 Copyright © 2000 by The Endocrine Society

Vol. 141, No. 2  
 Printed in U.S.A.

## Differential Effects of Insulin-Like Growth Factor (IGF)-Binding Protein-3 and Its Proteolytic Fragments on Ligand Binding, Cell Surface Association, and IGF-I Receptor Signaling\*

GAYATHRI R. DEVI†, DOO-HYUN YANG‡, RON G. ROSENFELD, AND YOUNGMAN OH

Department of Pediatrics, School of Medicine, Oregon Health Sciences University, Portland, Oregon 97231-3042

### ABSTRACT

Insulin-like growth factor (IGF)-binding protein-3 (IGFBP-3), the predominant IGF carrier protein in circulation, is posttranslationally modified *in vivo* by IGFBP-3 protease(s) into a number of fragments. Based on the ascertained and predicted recognition sites for known IGFBP-3 proteases, N-terminal epitope-tagged intact IGFBP-3, NH<sub>2</sub>-terminal (1–97), intermediate fragment (88–148), and COOH-terminal fragments (98–264 and 184–264) were generated in a baculovirus and/or *Escherichia coli* expression system and examined, by Western ligand blot and affinity cross-linking assays, for their ability to bind IGF and insulin. The NH<sub>2</sub>- and COOH-terminal fragments bound both IGF and insulin specifically (albeit with significantly reduced affinity) for IGF but higher affinity for insulin, when compared with intact IGFBP-3. The effect of IGFBP-3 and the fragments on IGF-I

receptor (IGFIR) signaling pathways was studied by testing IGF-I-induced receptor autophosphorylation in IGFIR-overexpressing NIH-3T3 cells. IGFBP-3 showed a dose-dependent inhibition of autophosphorylation of the β-subunit of IGFIR. The (1–87) NH<sub>2</sub>-terminal fragment inhibited IGFIR auto phosphorylation at high concentrations, and this effect seems largely attributable to sequestration of IGF-I. In contrast, no inhibition of IGF-I-induced IGFIR auto phosphorylation was detected with the (88–264) and (184–264) COOH-terminal fragments, despite their ability to bind IGF. However, unlike the (1–97) NH<sub>2</sub>-terminal fragment, the COOH-terminal fragments of IGFBP-3 retained their ability to associate with the cell surface, and this binding was competed by heparin, similar to intact IGFBP-3 (*Endocrinology* 141: 0000–0000, 2000).

THE INSULIN-LIKE GROWTH factors (IGF)-I and -II play an active role in cell proliferation and exist in association with distinct and specific IGF-binding proteins designated as IGFBPs 1–6 (1) and possibly IGFBP related proteins (IGFBP-rPs) (2). IGFBP-3, the major IGFBP in adult serum, binds both IGFs with high affinity and specificity, and it serves as a carrier of IGFs, prolonging their half lives, as well as modulating their proliferative and anabolic effects on target cells by regulating IGF bioavailability. Exogenous IGFBP-3 has also been demonstrated to significantly inhibit the growth of various cells, including, Hs578T estrogen receptor-negative human breast cancer cells (3). Decreased cell growth was observed when human IGFBP-3 complementary DNA (cDNA) was transfected into mouse Balb/c fibroblast cells (4) and into fibroblast cells derived from mouse embryos homozygous for a targeted disruption of the type 1 IGF receptor gene (5). The mechanism of this inhibition seems to

be both IGF-independent and IGF receptor-independent and is mediated, presumably, through binding to specific IGFBP-3 receptors (6–8).

IGFBP-3 may be posttranslationally modified by IGFBP-3 protease(s) present in biological fluids or culture media (plasmin, prostate-specific antigen (PSA), matrix metalloprotease) (9) and those whose activity has been demonstrated only *in vitro* like that of stromelysin 3, thrombin (10). Serum IGFBP protease(s) have been detected in diabetes (11, 12), renal (13), pregnancy (14), malignancy (15, 16), and following traumatic conditions or invasive procedures, such as surgery. Cleavage sites in IGFBP-3 have been located at the beginning of the variable domain (residues 95–98), particularly residue 97, which is the cleavage site for PSA, plasmin, human serum, and thrombin yields a fragment of approximately 16 kDa or 20 kDa (glycosylated IGFBP-3) (10). However, the C-terminal fragments, containing a highly basic heparin binding domain, have only been detected *in vitro* by plasmin digestion of intact IGFBP-3 and those fragments seem to inhibit degradation of other binding proteins (17). It is recognized that IGFBP proteolysis also occurs in the normal state outside of the bloodstream (18, 19) and that, in the cell environment, it is an essential mechanism in regulating the bioavailability of IGF. Both intact IGFBP-3 and IGFBP-3 proteolytic fragments have been shown to be capable of blocking the autogenic effect of IGFs (20). Whether these actions primarily represent IGF-independent or IGF-independent remains to be determined.

Received March 28, 2000.

Address all correspondence and requests for reprints to: Gayathri R. Devi, PhD, AVI Biopharma, Inc., 4575 SW Research Way, Suite 200, Corvallis, Oregon 97333. E-mail: gdevi@avibio.com.

\*This research was supported by US Army Grants DAMD17-99-1-0777 (to G.R.D.) and DAMD17-99-1-0204 and DAMD17-96-1-7204 (to Y.O.) and by NTT Grants R01-DK-51513 (to R.G.R.) and CA-98110 (to R.G.R.).

†Present address: AVI Biopharma Inc., 4575 SW Research Way, Suite 200, Corvallis, Oregon 97333.

‡Present address: Department of Surgery, Chonbuk National University Medical School, Chonju, Korea.

Orig. No.	OPERATOR:	Session	PROOF	PE's	AA's	COMMENTS	ARTNO:
1st disk, 2nd RWA	Editor	5	✓	✓			66000

JOBNAME: END (ee) PAGE: 2 SESS: 5 OUTPUT: Thu Aug 24 06:01:14 2000  
 /balt3/ee cnd/cc-end/eel100/ee77/01 USA

AUTHOR:  
 see query  
 in MS

## THE EFFECT OF IGFBP 3 FRAGMENTS ON IGFIR SIGNALING

Page 2 of 2000  
 Vol. 541-NR. 11

Our laboratories have demonstrated that the NH<sub>2</sub>-terminal recombinant fragments of IGFBP-3 (1-87) and (1-97) retain the ability to bind IGF-I with substantially reduced affinity. Additionally, these fragments specifically bind insulin and modulate insulin binding to its receptor (21, 22). Based on these studies, it has been hypothesized that the conserved NH<sub>2</sub>- and COOH-terminal sequences, as well as the appropriate ternary structure formed by disulfide bonds in the six classical IGFBPs, are all required for high-affinity binding of IGFs. A recent study had indicated that a natural COOH-terminal fragment of human IGFBP-2 retained partial IGF-binding activity (23), and a C-terminal, 13 kDa IGFBP-3 fragment (isolated from hemofiltrate) showed similar results (24). However, there is limited information on the binding characteristics of the IGFBP-3 COOH-terminal domain and the resultant biological effects of proteolytic fragments containing either the NH<sub>2</sub>- or COOH-terminal residues.

In this study, we demonstrate the ability of COOH-terminal fragments of IGFBP-3 to bind IGF-I. The (NH<sub>2</sub>-144)IGFBP-3 fragment and the (1-97)NH<sub>2</sub>-terminal fragment are both characterized, furthermore, by the ability to bind insulin with low affinity, but with higher affinity than is the case for intact IGFBP-3. Additionally, we have examined the effect of intact IGFBP-3 and the IGFBP-3 fragments on IGF-I-stimulated autophosphorylation of the IGF-I receptor (IGFIR) β-subunit and their ability to associate with the cell surface.

## Materials and Methods

## Antibodies and reagents

IGF-I and IGF-II were purchased from Axokal Biologicals (Santa Clara, CA). <sup>125</sup>I-ICF-I (specific activities between 50-70 μCi/μg) by a modification of chloramine-T technique and ICFFP-3 monoclonal antibody were kindly provided by Diagnostic Systems Laboratories, Inc., Webster, TX. IGFBP-3 cDNA was obtained from Celtrix Pharmaceuticals, Inc. (Santa Clara, CA). <sup>125</sup>I-(A14)-labeled insulin was purchased from Amersham Pharmacia Biotech. bovine insulin was purchased from Sigma. Antiphosphotyrosine monoclonal antibody (4G10) was a generous gift from Dr. B. J. Druker (Department of Hematology and Medical Oncology, Oregon Health Sciences University). Reagents used for SDS-PAGE were purchased from Bio-Rad Laboratories, Inc. (Richmond, CA).

## Cell culture

NH313 cells overexpressing the human IGFIR were kindly gifted from Dr. C. T. Roberts, Jr. (Department of Pediatrics, Oregon Health Sciences University) and grown in DMEM with 10% FCS plus 500 μg/ml genetin at 37°C with 5% CO<sub>2</sub>.

## Generation and purification of recombinant IGFBP-3 proteolytic fragments

(1-97)IGFBP-3 and (88-118)IGFBP-3 FLAG-epitope tagged fragments were generated and purified in baculovirus and tested to be 99% pure, as described earlier (25, 26). The cDNAs for the COOH-terminal fragments (98-264) and (184-264) were generated by PCR amplification from the human IGFBP-3 cDNA and a FLAG epitope sequence (DYKTDIDK), and a stop codon was added immediately following amino acid 264. The signal peptide sequences of IGFBP-3 cDNA were deleted to NH<sub>2</sub>-termini of IGFBP-3 fragments. After sequencing, the qPCR amplicon was then subcloned into the pectinavirus expression vector pFASTBAC1 (Life Technologies) and transformed into DH10Bac Escherichia coli. The amplified DNA was transfected into SF9 insect cells (ATCC), and large scale protein purification was begun by infecting the P2 virus into 10<sup>6</sup> HEK-293 cells (Invitrogen), at a multiplicity of infection of 3, at 27°C for 3 days. The media from the infected cells were

collected and concentrated, and the resultant were bound to anti-M2 antibody column overnight at 4°C, and the FLAG-tagged (98-264) protein was then eluted by using FLAG peptide (0.5 μg/ml), as described earlier (27). The purified protein was subjected to SDS-PAGE in a 15% gel and stained with Coomassie blue. Further, the fragment was also identified by immunoblotting with the M2 anti-FLAG antibody (Eastman Kodak Co., New Haven, CT) and anti-IGFBP-3 monoclonal antibody (Diagnostic Systems Laboratories, Inc.). Eluted fractions from anti-M2 antibody column were pooled, concentrated, and quantified by comparison with known amounts of BSA and IGFBP-3 standards after silver staining.

The (144-264)IGFBP-3 amplicon, after sequencing, was subcloned in the C-terminal end of glutathione S-transferase (GST) in the plasmid pGEXAT and transformed into *Escherichia coli* cells. The culture was grown overnight in L-Bam media and induced with 2 mM IPTG, and the cell lysates of the (144-264)GST fusion protein were prepared. The lysates were incubated with GST Sepharose beads for 1 h at RT and then washed. Purity and concentration of the fragments were determined by comparison with known amounts of BSA standards after silver staining. Further, the purified protein was subjected to SDS-PAGE in a 15% gel and stained with Coomassie blue and also transferred to nitrocellulose and identified by immunoblotting with M2 anti-FLAG antibody (1:2000 dilution).

## Affinity cross-linking

Intact IGFBP-3 or the NH<sub>2</sub>- and COOH-terminal fragments were incubated with <sup>125</sup>I-IGF-I or <sup>125</sup>I-insulin (50,000 cpm), in the presence or absence of unlabeled ligand, in a 100-μl vol for 16 h at 4°C and then cross-linked with 0.5 mM diisocyanimidyl suberate (DSS) for 15 min at 4°C. The samples were then subjected to SDS-PAGE (12% or 15% gels) under reducing conditions, and autoradiography on Biomax MS film (Eastman Kodak Co.). Bands were quantified by densitometry (Bio-Rad Laboratories, Inc.).

## Western ligand blot analysis

Ligand blotting was performed as described by Hoogenlopp et al (28), with minor modifications. Briefly, samples of intact IGFBP-3 (1-97), IGFBP-3, and (98-264)IGFBP-3 fragments, at the concentrations indicated in the figure legends, were subjected to SDS-PAGE (12% or 15% gel) under reducing or nonreducing conditions, electroblotted onto nitrocellulose filters, incubated with 1.5 × 10<sup>6</sup> cpm of <sup>125</sup>I-insulin or a mixture of <sup>125</sup>I-IGF-I and <sup>125</sup>I-IGF-II, washed, dried, and exposed to film (Biomax).

Monolayer <sup>125</sup>I-IGF-I affinity cross-linking

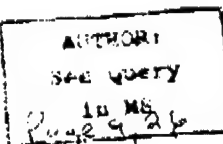
<sup>125</sup>I-IGF-I (100,000 cpm) was preincubated in a microfuge tube for 2 h at 4°C, in the presence or absence of cold IGF-I, intact IGFBP-3 (30 nM) (98-264), IGFBP-3 (250 nM) (144-264), IGFBP-3 (250 nM), or (1-97)IGFBP-3 (250 nM), in binding buffer (50 mM HEPES, 150 mM NaCl, 0.7% BSA). Confluent NH313-IGFIR cells stably transfected with the human IGFIR cDNA (NH313-IGFIR cells) were incubated in serum free medium overnight. The cells were washed once with PBS. The cells were incubated with the <sup>125</sup>I-IGF-I/IGFBP-3 combinations in triplicate wells for 1 h at 15°C. The cells were then washed with PBS and cross-linked with DSS for 15 min at 4°C, and the reaction was quenched with 100 mM Tris/HCl. The cells were solubilized with sample buffer. The covalent ligand-receptor (<sup>125</sup>I-IGF-I/IGFIR) complex in the lysates was resolved on a nonreducing 6% SDS-PAGE, followed by autoradiography. Another set of the same samples of cell lysates was run on a 15% SDS-PAGE under reducing conditions and immunoblotted with M2 anti-FLAG antibody or anti-IGFBP-3 monoclonal antibody, and the cell associated bands were detected with enhanced chemiluminescence (Amersham Pharmacia Biotech).

## Determination of cell surface association of intact IGFBP-3 and the fragments

Confluent monolayers of NH313-IGFIR cells were incubated in serum free medium overnight. Intact IGFBP-3 (30 nM), fragments (98-264) (250 nM), 144-264 (250 nM), or 1-97 (250 nM) in the presence or absence

Orig. No.	OPERATOR:	Section:	PROOF:	PE's:	AA's:	COMMENTS	ARTNO:
1st disk, 2nd 1WBS	Tullers	6	C 6/2				RSB009

JOURNALNAME: END (cc) PAGE: 3 SESS: 5 OUTPUT: Thu Aug 24 06:01:14 2000  
/bal3/cc-end/cc-end/cc1100/cc7781 00a



### THE EFFECT OF IGFBP-3 FRAGMENTS ON IGFIR SIGNALING

3

of 100  $\mu$ g/ml heparin (Sigma), in binding buffer, was added to the cells. In a similar experiment, cells were treated with heparin (100  $\mu$ g/ml) for 1 h, before addition of the peptides as listed above. The treatments were separated and at 15 °C for 3 h. The cells were washed with PBS and cross-linked with DSS, as described above. The solubilized cell lysates were then run on a 15% SDS-PAGE and immunoblotted with anti-IGFBP-3 monoclonal antibody and detected with enhanced chemiluminescence.

#### *IGF-I-induced IGFIR autophosphorylation assay*

Confluent monolayers of serum-starved NIH-3T3-IGFIR cells were exposed for 5 min to 7 nM IGF-I, which had been preincubated with/without intact IGFBP-3 (1–97), IGFBP-3 (98–264) or IGFBP-3 (88–264) for 2 h at 4 °C. The reaction was quenched by solubilization buffer [1% Nonidet P-40, 20 mM Tris-HCl (pH 8.0), 1 mM EDTA, 150 mM NaCl, 10% glycerol, 12 U/ml aprotinin, phenylmethylsulfonyl fluoride, and 1 mM Na<sub>3</sub>VO<sub>4</sub>]. Solubilized proteins (25  $\mu$ l of the cell lysates) were separated by SDS-PAGE (7.5%) under reducing conditions and visualized by immunoblot analysis. For immunoblot analysis, the filters were blocked in Tris-buffered saline (TBS) with 2% gelatin for 1 h at room temperature and then incubated with antiphosphotyrosine monoclonal antibody (1.5  $\mu$ g/ml) diluted by TBS + 0.1% Triton X-100 (TBST) for 1 h at room temperature. The filters were then rinsed in 1  $\times$  TBST and incubated in a 1:5000 dilution of goat antimouse IgG-conjugated horseradish peroxidase (Amersham Pharmacia Biotech) for 1 h at room temperature. Immunoreactive protein were visualized using an enhanced chemiluminescence detection system.

#### Results

##### *Expression of the IGFBP-3 recombinant fragments*

Based on the ascertained and predicted YSA recognition sites in IGFBP-3 and the recognition sites for other known IGFBP-3 proteases, such as metalloproteases and plasmin, both intact IGFBP-3 and four different recombinant fragments were generated in a baculovirus and/or *Escherichia coli* expression system. Each peptide was coupled with a FLAG epitope tag at the carboxyterminus, as shown in Fig. 1A. The purified proteins were immunoblotted with anti-FLAG M2 or anti-IGFBP-3 monoclonal antibody for estimation of their molecular weights. Intact IGFBP-3 and all the fragments were detectable by anti-FLAG M2 antibody under reducing (Fig. 1B) and nonreducing conditions. Dimerized forms of the proteins were identified in anti-FLAG M2 immunoblots run under nonreducing conditions (data not shown). Small discrepancies between the Mr for intact IGFBP-3 (1–97), IGFBP-3 (98–264), (IGFBP-3, and (88–148)IGFBP-3 proteins seen on the immunoblots relative to the predicted Mr, which is purely based on amino acid composition of the proteins, may have arisen because of N-linked glycosylation. There are three potential N-glycosylation sites (Fig. 1A): Asn<sup>99</sup>, Asn<sup>109</sup>, and Asn<sup>144</sup>, in IGFBP-3 (29). The anti-IGFBP-3 monoclonal antibody detected intact IGFBP-3 and (98–264)IGFBP-3 under both nonreducing (Fig. 1B) and reducing conditions (data not shown). The fragment 1–97 was detectable only under nonreducing conditions. The 148–264 and 88–148 fragments were not detected effectively with this antibody.

##### *Analysis of IGF binding to the IGFBP-3 proteolytic fragments*

To determine whether the regions encompassed by the IGFBP-3 fragments contained a functional R,I,L-binding/cross-linking site, the proteins were incubated with <sup>125</sup>I-IGF I and then affinity cross-linked with DSS and analyzed by SDS-PAGE. The data in Fig. 2A demonstrate that <sup>125</sup>I-IGF I

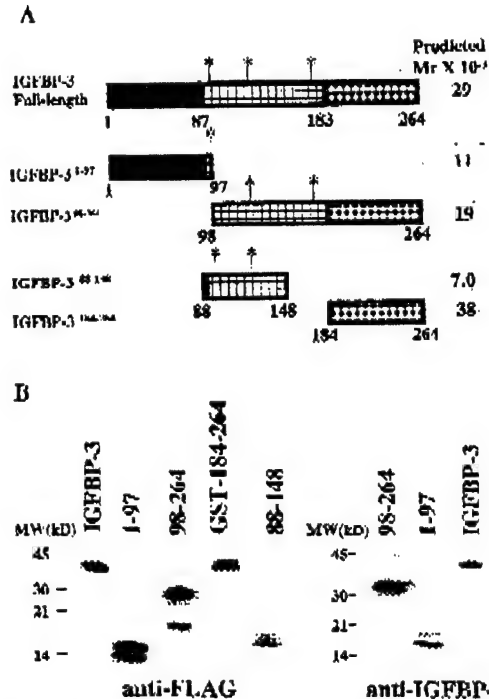


FIG. 1. Expression of FLAG-epitope tagged human IGFBP-3 and its fragments. A, The cDNA for preparation of the IGFBP-3 fragments was synthesized by a series of PCR reactions using the human IGFBP-3 cDNA as template and incorporating sequence encoding a COOH-terminal FLAG epitope tag. The dark boxes (1–97) represent the conserved NH<sub>2</sub>-terminal region; the diamond striped boxes (183–284), the conserved COOH-terminal region; and the square striped boxes (88–148), the variable intermediate region of IGFBP-3. The predicted molecular weights (MW) are based on the amino acid composition of the proteins. B, Protein expression was analyzed by immunoblotting using the M2 monoclonal antibody under reducing conditions or the IGFBP-3 monoclonal antibody under nonreducing conditions, coupled to ECL.

can be cross-linked to the (1–97)IGFBP-3 and (98–264)IGFBP-3 fragments in a dose-dependent manner. Significant IGF cross linking was observed at 50 nM concentrations of (1–97)IGFBP-3, which was completely saturated by 100 nM concentrations. In the case of (98–264)IGFBP-3, a dose-dependent increase in IGF binding with increasing protein concentrations with saturation of binding occurred by 500-nM concentration range. The expected sizes of the individual proteolytic fragment coupled to <sup>125</sup>I-IGF I were detected, shown as 25 and 41 kDa bands, respectively. A faint band at 39 kDa is potentially a dimerized form of 1–97 fragment cross-linked to IGF-I.

For estimation of the affinity of IGF-I binding, the proteolytic fragments were affinity cross-linked with <sup>125</sup>I-IGF I in the presence of increasing amounts of unlabeled IGF-I or

Only On	OPERATOR:	Session	PROTOTYPES:	AA's:	COMMENTS	ARTNO:
1st disk, 2nd HWB	tulera	6	(5) 147			WBW000

ATTACH  
See query  
D 10 MS  
20-17

## THE EFFECT OF IGFBP-3 FRAGMENTS ON IGFIR SIGNALING

5

*Analysis of insulin binding to IGFBP-3 fragments*

The observations that insulin could compete for  $^{125}\text{I}$ -IGF-I binding to the fragments led us to assess their insulin binding activity. Both (1-97)IGFBP-3 and (98-264)IGFBP-3 showed a strong  $^{125}\text{I}$ -insulin cross-linking band, in comparison with that observed with IGFBP-3 at similar concentrations (Fig. 4a). Unlabeled insulin was able to dose-dependently inhibit  $^{125}\text{I}$ -insulin binding to both the NH<sub>2</sub> and COOH-terminal fragments (Fig. 4b), although even higher concentrations of unlabeled insulin could not completely displace  $^{125}\text{I}$ -insulin binding to the (98-264)IGFBP-3, suggesting a slow dissociation rate. Calculation of the unlabeled insulin concentrations required to achieve IC<sub>50</sub> indicated that the (1-97)IGFBP-3 had an IC<sub>50</sub> value ranging between 0.3-0.4  $\mu\text{M}$ , whereas nearly 1  $\mu\text{M}$  unlabeled insulin was required to cause 50% displacement of  $^{125}\text{I}$ -insulin binding to the (98-264) fragment (Fig. 4c). IGF-I was also able to compete for the  $^{125}\text{I}$ -insulin binding to the fragments, although higher concentrations of IGF-I were required in the case of (98-264)IGFBP-3. In summary, the (1-97)IGFBP-3 showed significantly high affinity for insulin, relative to the (98-264)IGFBP-3 fragment.

Further, Western blot analysis with iodinated insulin showed that both the 1-97 and the 98-264 fragments bound insulin. The IGFBP-3 intermediate fragment (88-148), which lacks both the NH<sub>2</sub>- and COOH-terminal domains, showed no binding to IGF-I, IGF-II, or insulin, in Western ligand blot (data not shown).

*IGFII and 1-97 fragments inhibit IGF-I interaction with the IGFIR*

To determine whether the ability of intact IGFBP-3 and the amino- and carboxyterminal fragments to bind IGFs *in vitro* lead to sequestration of IGFs *in vivo*, a  $^{125}\text{I}$ -IGF-I monolayer affinity cross-linking assay was done in the NIH 3T3 cells overexpressing the IGFIR (NIH-3T3-IGFIR). The data in Fig. 5A shows that  $^{125}\text{I}$ -IGF-I specifically cross-links with the IGFIR shown as a 230-kDa band under nonreducing conditions.  $^{125}\text{I}$ -IGF-I binding to IGFIR was completely displaced by 100 nM unlabeled IGF-I. Further, the IGF-I-IGFIR complex formation was completely inhibited by preincubation of the iodinated IGF-I with unlabeled IGFBP-3 (10 nM) and about 90% inhibited by preincubating with 250 nM concentration of (1-97) NH<sub>2</sub>-terminal fragment. The cross-linked band was not inhibited, however, by preincubation of the  $^{125}\text{I}$ -IGF-I with 250 nM of (98-264)IGFBP-3 or the (184-264)IGFBP-3 fragment.

The same set of samples were resolved on an immunoblot and probed with M2 anti-IGF-II antibody. Results in Fig. 5B show that the carboxyterminal fragments (98-264), (184-264), and intact IGFBP-3 molecules associated with the cell surface in the presence of IGF-I. (1-97)IGFBP-3, however, showed no cell-associated band.

*The carboxyterminal fragments have the ability to associate to the cell surface*

Because, compared with the NH<sub>2</sub>-terminal fragment, the (98-264) COOH-terminal IGFBP-3 fragment failed to inhibit binding of IGF-I to the IGFIR, we wanted to study the ability

of the fragments to associate with the cell surface in the absence of IGF-I. Monolayer cross linking was carried out with the PLAC epitope tagged Intact IGFBP-3 (1-97) or (98-264) fragments in NIH-3T3-IGFIR cells, and the cell-associated proteins were detected by immunoblotting the cell lysates with anti-IGFBP-3 monoclonal antibody. The (98-264) carboxyterminal fragment and intact IGFBP-3 molecules associated with the cell surface (1-97)IGFBP-3, however, showed no cell-associated band (Fig. 6, lanes 2 and 5). Further, there was no detectable shift in molecular weights of the cross-linked proteins when compared with control (Fig. 1B) noncross-linked protein preparations.

To test whether the ability of intact IGFBP-3 and the carboxyterminal fragment to bind to the cell surface was via the heparin-binding domain, cells were preincubated with heparin (100  $\mu\text{g}/\text{ml}$ ) and then treated with the peptides; alternatively, the peptides were preincubated with heparin and then added to the cells followed by monolayer cross-linking in both cases (Fig. 6). Similar results were observed in both types of experiments, i.e. heparin blocked the cell surface association of intact IGFBP-3 (Fig. 6, lanes 3 and 4) and the (98-264)IGFBP-3 fragment (Fig. 6, lanes 6 and 7).

*Inhibition of IGFIR signaling*

Because intact IGFBP-3 and its fragments have the ability to bind IGFs and thereby impede its interaction with the IGFIR, we analyzed the potential biological manifestation of this interaction on IGFIR signaling. This was carried out by testing the effect of IGFBP-3 and its fragments on IGF-I-induced IGFIR autophosphorylation in NIH-3T3-IGFIR cells. Control experiments with IGF-I revealed that 5-min treatments with 7-14 nM of the peptide showed maximal intensity autophosphorylation of the 95-kDa band of the  $\beta$ -subunit of IGFIR in antiphosphotyrosine immunoblots (Fig. 7A).

IGFBP-3 inhibited IGF-I stimulated autophosphorylation of the IGFIR  $\beta$ -subunit in a dose-dependent manner (Fig. 7B). Quantification of the inhibition of the phosphorylated subunit of IGFIR was carried out by densitometrically analyzing the specific 95 kDa band and the 116 kDa nonspecific band in each gel. The ratio of the two band intensities was used to normalize and calculate the percentage of maximal IGF-I-stimulated IGFIR autophosphorylation detected in the presence of IGFBP-3 and the IGFBP-3 fragments (Fig. 7C). IGFBP-3 caused 50% inhibition of the IGF-I-induced autophosphorylation at >7 nM concentration range, and by 15-20 nM IGFBP-3 concentrations, complete inhibition of IGFIR autophosphorylation was observed. In contrast, the (1-97)IGFBP-3 fragment inhibited receptor autophosphorylation only at higher concentrations (40-70% inhibition at 110-250 nM concentrations). The (98-264)IGFBP-3 and (184-264)IGFBP-3 fragments, however, did not show any significant inhibition of IGF-I-induced IGFIR autophosphorylation, even at 250 nM concentrations (Fig. 7, B and C), although these fragments were able to bind IGF-I in binding assays.

*Discussion*

We report herein that IGFBP-3 fragments are capable of binding IGF-I and IGF-II, although with lower affinity than that seen with intact IGFBP-3. Further, the fragments have

Orig. Op.	OPERATOR:	Session	PROOF	Pts:	M's:	COMMENTS	ARTNO:
1st disk, 2nd PWS	fillers	5	13				858089

## THE EFFECT OF IGFBP-3 FRAGMENTS ON IGFIR SIGNALING

Vol. 24, No. 11

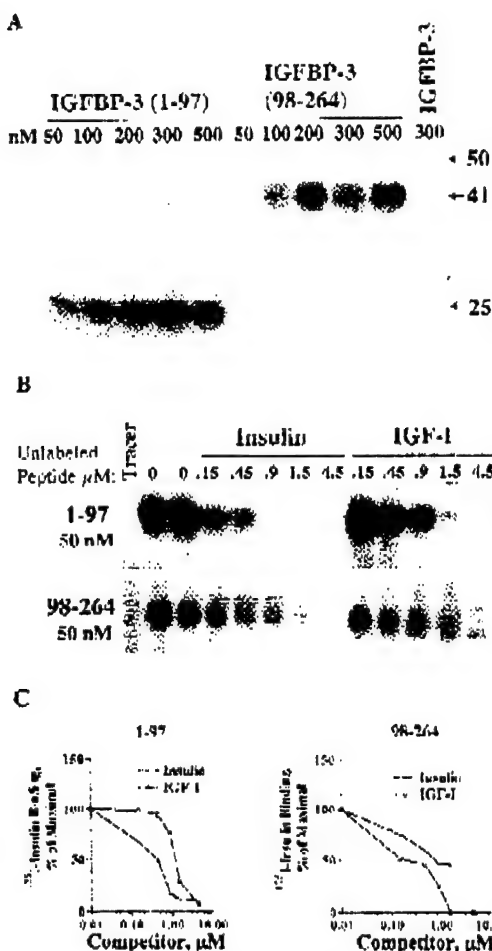


**FIG. 4.** Insulin binding analysis. **A**,  $^{125}\text{I}$ -insulin affinity cross-linking. IGFBP-3 proteolytic fragments were incubated with  $^{125}\text{I}$ -insulin ( $1 \times 10^6 \text{ cpm}$ ) in a  $100 \mu\text{l}$  vol for 16 h at 4°C and then cross-linked with 0.5 mM DSS for 15 min at 4°C. The affinity labeled fragments were separated on a 15% SDS polyacrylamide gel. An autoradiogram of the gel is shown, which is representative of three replicates. Values associated with the arrows indicate the calculated molecular weights of the major radioactive species. **B**, Competitive  $^{125}\text{I}$ -insulin affinity cross-linking: IGFBP-3 and the proteolytic fragments (50 nM) equivalent to 6 nmol were incubated with radiolabeled insulin in the presence or absence of the indicated concentrations of unlabeled insulin or IGF-I. Cross-linking was then done with DSS, followed by SDS-PAGE. The autoradiogram of the dried gel is shown. The arrows indicate the major radioactive species. **C**, Quantitative analysis of radiolabelled  $^{125}\text{I}$ -insulin displacement from IGFBP-3 fragments: the gels shown in **B** were densitometrically analyzed for quantitative estimation of the radioactivity associated with the individual bands. The data have been expressed as a percentage of maximal band intensity.

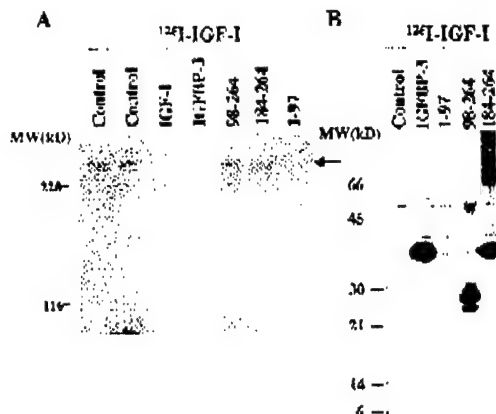


**FIG. 5.** Monolayer affinity cross-linking with  $^{125}\text{I}$ -IGF-I. **A**,  $^{125}\text{I}$ -IGF-I was preincubated at 4°C in the presence or absence of unlabeled IGF-I (100 nM), IGFBP-3 (30 nM), or fragments (350 nM); and then these treatments were added to confluent monolayer of NIH 3T3 IGFIR cells for 3 h at 15°C. After washing, the cells were cross-linked, and cell lysates were run on a 15% SDS PAGE gel. The arrow indicates the IGFIR-specific cross-linked to radiolabeled IGF-I. **B**, A set of the same cell lysates were run on a 15% SDS PAGE, under reduced conditions, and immunoblotted with M2 anti FLAG monoclonal antibody.

the ability to bind insulin with higher affinity than observed with intact IGFBP-3. The principal conclusion is that the high affinity binding of IGFs by IGFBP-3 requires proper tertiary configuration of the NH<sub>2</sub>- and COOH-terminal domains. This observation is further supported by the recent concept of an IGFBP superfamily (31,32). Over the course of evolution, the classical IGFBPs, which have well conserved NH<sub>2</sub>- and COOH-terminal domains, evolved into high-affinity IGF-binders (1). In contrast, the IGFBPs (low-affinity IGFBPs) only share the conserved NH<sub>2</sub> terminal domain (32). This structural difference, combined with the present data, strongly implicate the importance of the IGFBP COOH-terminal domain in conferring high-affinity IGF binding.

The concept that interaction between NH<sub>2</sub>- and COOH-terminal domains is essential for high-affinity IGF binding was initially conceived based on observations that proteolysis of IGFBPs in biological fluids results in fragments that have diminished or no binding affinities for IGFs (33). The *in vitro* generation of recombinant fragments or fragments isolated by limited proteolysis supports the *in vivo* data. A 16-kDa fragment corresponding to the NH<sub>2</sub> terminus and a small portion of intermediate region, generated by proteolytically modifying IGFBP-4, specifically cross-linked to both IGF-I and II, although with a 20-fold lower affinity than intact IGFBP-4 (34,35). Similarly, a carboxy-truncated 23-kDa IGFBP-5 fragment from osteoblast-like cells demonstrated decreased IGF binding affinity (36,37). Deletion mutagenesis of the carboxyterminal domains of IGFBP-1 and IGFBP-4 has resulted in a decrease in IGF affinity, thereby demonstrating the importance of the highly conserved Lys-Tyr-Lys-Val motif in the carboxyterminal region (38,39). The present study

Org. Op.	OPERATOR	Session	PROOF	PE%	AA%	COMMENTS	ARTNO:
1st disk, 2nd RWB	Jullens	5					058080

## THE INFLUENCE OF IGFBP FRAGMENTS ON IGFIR SIGNALING

7

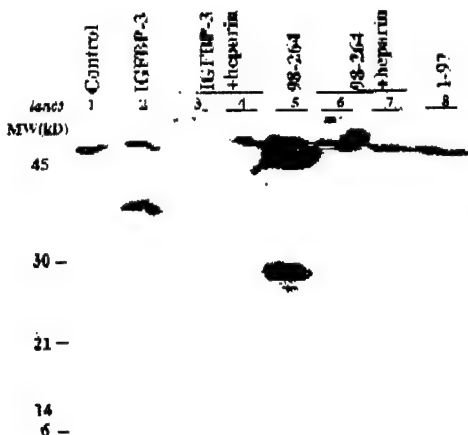


**Fig. 8.** Effect of heparin on cell surface association of IGFBP-3 and its fragments. Confluent NIH 3T3-IGFIR cells were treated with either peptides alone [lane 1, untreated cells; lane 2, IGFBP-3; lane 5, (98-264)IGFBP-3; lane 6, (1-97)IGFBP-3] or with peptides preincubated with heparin for 1 h at 4°C [lane 4, IGFBP-3+heparin; lane 7, (98-264)IGFBP-3+heparin]; or the cells were first treated with heparin for 1 h, washed, and then the following peptides were added: lane 8, IGFBP-3; lane 9, (98-264)IGFBP-3. All the treatments were carried out for 3 h at 16°C. After washing, the cells were cross-linked, and cell lysates were run on a 15% SDS PAGE and immunoblotted with anti-IGFBP-3 monoclonal antibody. The arrows indicate the cell-surface-associated species.

is the first to clearly demonstrate the ability of the 28-kDa (98-264), IGF-I/II<sup>1</sup>-intermediate COOH-terminal proline-rich fragment to bind both IGFs and insulin in two different procedures, affinity cross-linking and Western ligand blot. Interestingly, the binding of the (98-264)IGFBP-3 fragment to <sup>125</sup>I-IGF-I or <sup>125</sup>I-insulin was competitively displaced by both IGF-I and insulin, though with different affinities, suggesting that the insulin and IGF binding sites are probably not identical but overlap or reside closely on the IGFBP-3 molecule. This is in contrast with the (1-97)IGFBP-3 fragment, where insulin and IGF-I were approximately equipotent in displacing <sup>125</sup>I-IGF-I.

We have shown that IGFBP-3 causes a dose-dependent inhibition of IGF-I-induced IGFIR autophosphorylation in NIH 3T3 cells overexpressing the IGFIR. This inhibition occurs at an 1.1 molar ratio of IGFBP-3 to IGF-I, suggesting an IGF-dependent mechanism of modulation of receptor signaling. The (1-97) NH<sub>2</sub>-terminal fragment retained the ability to modulate IGF-I binding and signaling via the IGFIR by inhibiting IGF-I-stimulated IGFIR autophosphorylation, albeit at 50-fold higher concentrations than intact IGFBP-3. That this inhibition of IGFIR signaling is largely attributable to sequestration of IGF-I is strongly supported by the observations that both intact IGFBP-3 and (1-97)IGFBP-3 compete with <sup>125</sup>I-IGF-I binding/cross-linking to the receptor in monolayer affinity cross-linking experiments.

Interestingly, the (98-264) fragment, unlike the (1-97) IGFBP-3, failed to show any inhibition of IGFIR signaling, despite its ability to bind IGFs, as revealed by *in vitro* binding

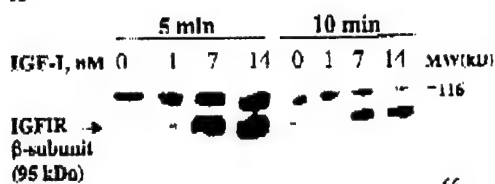
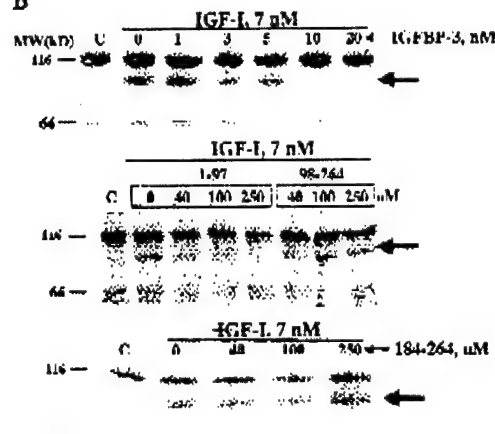
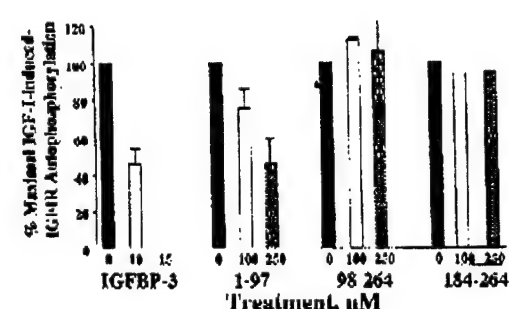
analysis. The COOH-terminal fragments (98-264) and (181-264) also failed to compete for <sup>125</sup>I-IGF-I binding and cross-linking to the IGFIR, compared with intact IGFBP-3 and the (1-97) NH<sub>2</sub>-terminal IGFBP-3 fragment. We speculate that the inability of the fragments containing the COOH-terminal domain of IGFBP-3 to inhibit IGF-I binding to the IGFIR could be attributable to the following mechanisms: 1) the COOH-terminal fragment binds IGF-I, and the entire complex is still capable of binding to and autophosphorylating the IGFIR, implying that the binding site on IGF-I for the receptor and for the carboxyterminal region of IGFBP-3 are different; and 2) the COOH-terminal domain of IGFBP-3 possesses an extracellular matrix (ECM) binding region, and it is possible that in the cellular environment, the fragments containing the COOH-terminal domains are more prone to associate with the cell surface and are not available to sequester IGF-I, especially given their low affinity for IGF-I. To test these hypotheses, the ability of the FLAG epitope-tagged fragments to associate with the cell surface was studied in the presence of IGF-I, with subsequent cross-linking and by analysis of cell lysates on immunoblot probed with anti-IGFBP-3 or M2 anti-IGF-I antibody. Our data indicate that the COOH-terminal fragments (98-264) and (181-264) have the ability to associate to the cell surface in the presence of IGF-I, unlike the NH<sub>2</sub> fragment (1-97), IGFBP-3, which showed no cell-surface association. Further, there was no shift in molecular weight of the cell-surface-associated bands, and heparin blocked the binding of both intact and the (98-264)IGFBP-3 fragment to the cell surface, ruling out the possibility of interaction of the fragments with any receptor molecule and thereby supporting the second hypothesis. This is in agreement with an earlier study (40), which reported that an IGFBP-3 deletion fragment, lacking the 184-264 region, failed to show any cell-surface association. There are two putative heparin-binding motifs in IGFBP-3, located at amino acids 148-153 and 219-226 in the central and carboxyterminal regions, respectively, and the carboxyterminal motif has been shown to have 4 fold higher affinity for heparin (41). Recently, Bramard *et al.*, 1999 (42), have identified two nonbasic residues (Gly111 and Glu119) within the ECM binding region (201-218) in the carboxyterminal region of IGFBP-3, mutations of which cause 8-10-fold reduction in affinity for human IGF-I. This region is a highly conserved domain in IGFBP-3, -5, and -6 and is known to contain the heparin-binding domain. The authors have proposed that the IGF-I and ECM binding sites partially overlap, and heparin binding to the basic amino acids might interfere with IGF-I interaction *in vivo*.

Previous studies with mini-receptor constructs and with isolated domains or proteolytic fragments of the IGF-II (43) urokinase receptor (44), GH receptor (45), tollin (46), to name a few, have confirmed the involvement of two or more ligand contact regions. Similarly, in the case of IGFBP-3, it seems that the IGF- and insulin-binding domains are bipartite and possibly overlapping. In our biological system, the stoichiometry of IGFBP-3 binding to IGF-I seems to be 1:1. We postulate that both NH<sub>2</sub>- and COOH-terminal domains have residues that are capable of binding IGF-I and insulin with low affinity. However, there is simultaneous interaction of the two so-called half-sites, in intact IGFBP-3, which creates a high-affinity IGF binding site on the molecule. Simultaneously, this interaction leads to a markedly reduced ability

Prog. No.	OPERATOR:	Session	TIME:	Pers:	Mrs:	COMMENTS	ARTNO:
1st disk, Prog 1WB	fullers	5	10:11				858089

## THE EFFECT OF IGFBP-3 FRAGMENTS ON IGFIR SIGNALING

Vol. 141 • No. 11

**A****B****C**

**Fig. 7.** IGFIR autophosphorylation assay. **A,** Confluent NIH 3T3-IGFIR cells stably transfected with the human IGFIR cDNA were exposed for either 5 min or 10 min to 1, 7, and 14 nM IGF-I peptide. The reaction was quenched by cold lysis buffer, and the solubilized proteins were separated by 7.5% SDS-PAGE under reducing conditions, and visualized by immunoblot analysis using anti-phosphotyrosine monoclonal antibody. The arrow indicates the 95 kDa  $\beta$ -subunit of IGFIR in each immunoblot. **B,** Confluent NIH 3T3-IGFIR cells were exposed for 5 min to 60 nM IGF-I, which had been preincubated with IGFBP-3, 1-17, or 98-264 proteolytic fragment for 2 h at 4°C. The

solubilized proteins were separated by 7.5% SDS-PAGE, under reducing conditions, and visualized by immunoblot analysis using anti-phosphotyrosine monoclonal antibody. The arrow indicates the 95 kDa  $\beta$ -subunit of IGFIR in each immunoblot. **C,** The specific 95-kDa bands representing the phosphorylated  $\beta$ -subunit of the IGFIR and the 116-kDa nonspecific bands in the gels shown in **B** and in other replicate experiments ( $n = 2-4$ ) were densitometrically analyzed. The ratio of the two band intensities was used to normalize and quantify the percentage of maximal IGF-I-induced IGFIR autophosphorylation detected in the presence of intact IGFBP-3 and its fragments.

In summary, the present study, along with previous work from our and other laboratories, clearly demonstrates the ability of the IGFBP-3 aminoterminal fragment to bind IGF and insulin and to inhibit IGFIR and insulin receptor auto-phosphorylation (21, 22), revealing that this 16-kDa fragment may be capable of both IGF-I-dependent and IGF-independent roles in modulating cell growth. However, the carboxyl-terminal fragments, which also have the ability to bind both IGF-I and insulin *in vitro*, fail to prevent binding of either IGF-I or insulin (data not shown) to their respective receptors, because of the tendency of these fragments for cell surface association via the heparin binding domain. Also intriguing is the identification of a thyroglobulin-like motif in the C-terminal regions of IGF-III superfamily, which has also been found in the superfamily of protein inhibitors of cysteine proteinases (47, 48). Whether this highly conserved thyroglobulin type-I element indeed acts as an inhibitor of cysteine proteinases in these proteins, remains to be established. The intermediate region of IGF-III does not seem to bind IGFs or insulin, and its role in high-affinity binding to IGFs is probably related to its ability to promote proper tertiary structure and optimal interactions between the amino- and carboxylterminal residues. Further, it has been demonstrated that the intermediate region of IGFBP-3 is involved in the specific interaction between IGF-III and its putative cell-surface receptor (26). Taken together, it is tempting to speculate that various forms of IGFBP-3 fragments resulting from proteolysis by IGFBP-3 specific proteases will have different effects on the IGF-IGFIR axis, as well as potential IGF-independent actions.

## Acknowledgments

We are grateful to Dennis Galloway and Elizabeth Wilson for technical support and to Drs. Victoria Hwa and Stephen M. Twigg for helpful

solubilized proteins were separated by 7.5% SDS-PAGE, under reducing conditions, and visualized by immunoblot analysis using anti-phosphotyrosine monoclonal antibody. The arrow indicates the 95 kDa  $\beta$ -subunit of IGFIR in each immunoblot. **C,** The specific 95-kDa bands representing the phosphorylated  $\beta$ -subunit of the IGFIR and the 116-kDa nonspecific bands in the gels shown in **B** and in other replicate experiments ( $n = 2-4$ ) were densitometrically analyzed. The ratio of the two band intensities was used to normalize and quantify the percentage of maximal IGF-I-induced IGFIR autophosphorylation detected in the presence of intact IGFBP-3 and its fragments.

Orig. Op.	OPERATOR:	Session	PROOF:	PE's AA's:	COMMENTS	ARTNO:
1st disk, 2nd RWS	dkies	5	-			050009

JOURNALNAME: END (cc) PAGE: 9 SDSS: 5 OUTPUT: Thu Aug 24 08:01:14 2000  
 /balt3/ee-end/ee-end/ee1103/eet781.00a

APPROVED
See Query
LA MS
Aug 21 2003

## THE EFFECT OF IGFBP-3 FRAGMENTS ON TGF $\beta$ 1 SIGNALING

D

discussions. We thank Diagnostic Systems Laboratories, Inc. for providing radiolabeled TGF $\beta$ .

### References

- Isaacs J, Clemons DK 1995 Insulin-like growth factors and their binding proteins: biological actions. *Endocr Rev* 16:23-34
- Rosenfeld RG, Iwasa V, Wilson L, Lopez-McNelly A, Buckley C, Burns C, Choi WK, Davis G, Ingemann A, Graven J 1993 The insulin-like growth factor binding protein superfamily. *Rev Respiratory Disease* 148:128-132
- Oh Y, Muller RL, Lemoine C, Rosenfeld KG 1993 Insulin-like growth factor (IGF)-independent action of IGF-binding protein-3 in MCF-7T human breast cancer cells. *J Biol Chem* 268:14904-14911
- Cohen P, Lamson G, Okajima T, Rosenfeld KG 1995 Transformation of the human K-Ras<sup>b12</sup> gene into NIH3T3 fibroblasts: a model for the cellular functions of IGFBPs. *Growth Regul* 5:3-76
- Valentini B, Blaikie D, DeAngelis T, Baserga R, Cohen P 1995 The human insulin-like growth factor (IGF) binding protein 3 inhibits the growth of fibroblasts with a targeted disruption of the K-Ras<sup>b</sup> receptor gene. *Mol Endocrinol* 9:661-667
- Oh Y, Muller RL, Pham H, Rosenfeld RG 1993 Demonstration of receptors for insulin-like growth factor binding proteins 3 in MCF-7T human breast cancer cells. *J Biol Chem* 268:29485-29488
- Rajah R, Valentini B, Cohen P 1997 Insulin-like growth factor (IGF) binding protein 3 induces apoptosis and mediates the effects of transforming growth factor- $\beta$ 1 on programmed cell death through a p53- and MAPK-independent mechanism. *J Biol Chem* 272:12101-12106
- Leal SM, Liu Q, Huang JS, Lee J 1997 Type V transforming growth factor- $\beta$  receptor is the putative insulin-like growth factor-binding protein 3 receptor. *J Biol Chem* 272:20742-20746
- Rajah R, Katz L, Nusin S, Selberg P, Hevesi T, Cohen P 1995 Insulin-like growth factor binding protein (IGFBP-3) promotes functional regulation of cell growth. *Prog Growth Factor Res* 6:775-782
- Bauml RA, Biava M, Bar RS 1996 KTF101-3 proteolysis by plasmin, thrombin, serine-heparin binding, KTF-binding and structure of fragment. *Am J Physiol* 271:L605-L610
- Heng P, Robinson K, Rosenfeld RG 1994 In vitro proteolysis of insulin-like growth factor-binding protein 3 (IGFBP-3) in semistarvation dependent diabetes mellitus serum, with elevation of a 29-kilodalton (kDa) glycosylated IGFBP-3 fragment contained in the approximately 138- to 150-kDa ternary complex. *J Clin Endocrinol Metab* 135:1119-1127
- Borkakoti A, Liang CH, Blethen SL, Fan J, Frost RA, Wilson TA 1995 Insulin-like growth factor binding protein-3 proteolysis in children with insulin-dependent diabetes mellitus: a possible role for insulin in the regulation of IGFBP-3 protease activity. *J Clin Endocrinol Metab* 136:2282-2288
- Powell DR, Durham SK, Lin P, Baker RK, Lee PD, Watkins ST, Campbell PG, Brown ED, Hind RI, Higgs RJ 1990 The insulin-like growth factor axis and growth in children with chronic renal failure: a report of the Southwest Pediatric Nephrology Study Group. *J Clin Endocrinol Metab* 131:161-166
- Bang P, Walter PJ 1997 Human pregnancy serum contains at least two different proteolytic activities with the ability to degrade insulin-like growth factor binding protein 3. *Endocrinology* 138:9912-9917
- Muller RL, Oh Y, Gospodarowicz DK, Wilson LF, Leiberman S, Rosenfeld RG 1994 Transforming growth factor- $\beta$ 1 binding protein-3, insulin-like growth factor binding protein 3 protease activity in sera of patients with malignant solid tumors or leukemia. *Pediatr Res* 35:720-724
- Romashka M, Romashka M, Gerasimov E, Faver R, Saithe D, Ponomarenko G 1995 Insulin-like growth factor (IGF) binding protein 3 (IGFBP-3) proteolysis in patients with colorectal cancer: positive association with the metastatic potential of the tumor. *J Clin Oncol* 13:467-470
- Ullman M, Lalou C, Mohseni-Zadeh S 1999 Biological actions of proteolytic fragments of the K-Ras<sup>b</sup>. In: Rosenfeld KG, Jr., Liao L, (eds) *The IGF System-Molecular Biology, Physiology, and Clinical Applications*. Humana Press, pp 281-313
- Lalou C, Ullman M 1993 Evidence that limited proteolysis of insulin-like growth factor binding protein 3 (IGFBP-3) occurs in the normal state outside of the bloodstream. *Regul Pept* 46:179-185
- Maili L, Xu S, Cwynar-Hughes SC, Ferrelli-JK, Belli JM, Holly JM 1991 Active and inhibitory components of the insulin-like growth factor binding protein-3 protease system in adult serum, intestinal, and synovial fluid. *Proteolysis* 139:1772-1781
- Lalou C, Lacoste C, Blaoux M 1994 A proteolytic fragment of insulin-like growth factor (IGF) binding protein-3 that fails to bind IGFs inhibits the mitogenic effects of K-Ras<sup>b</sup> and insulin. *Endocrinology* 135:3206-3212
- Yamamoto Y, Wilson EA, Rosenfeld KG, Oh Y 1994 Inhibition of insulin receptor activation by insulin-like growth factor binding protein-3. *J Biol Chem* 277:30790-30794
- Yamamoto Y, Yamada A, Oh Y, Rosenfeld RG 1996 Insulin and KTF binding by IGFBP-3 fragments derived from proteolysis, exclusive expression and normal human urine. *J Clin Endocrinol Metab* 133:1592-1595
- Oh P, Baker RC 1992 Characteristics of truncated insulin-like growth factor-binding protein-3 in human milk. *Endocrinology* 133:6011-6016
- Standköt L, Wohlf P, Mark S, Eisenmann WG 1998 Isolation and characterization of circulating 10-kDa C-terminal fragments of human insulin-like growth factor-binding protein-3. *FEBS Lett* 411:281-286
- Vorwerk D, Oh Y, Lee PD, Khare A, Rosenfeld KG 1997 Synthesis of IGFBP-3 fragments in a baculovirus system and characterization of monoclonal anti-IGFBP-3 antibodies. *J Clin Endocrinol Metab* 82:3268-3270
- Yamamoto Y, Privalov JL, Rosenfeld RG, Oh Y 1999 Characterization of insulin-like growth factor binding protein 3 (IGFBP-3) binding to human breast cancer cells. *Endocrinology* 140:1109-1112
- Oh Y, Nagata SR, Yamamoto Y, Klein H-S, Wilson E, Rosenfeld RG 1996 Synthesis and characterization of insulin-like growth factor binding protein (IGFBP-7). *J Biol Chem* 271:30322-30325
- Hogenboom P, Beurne U, Begovac-Gromica B, Hardouin S, Bindra M 1986 Analysis of serum insulin-like growth factor binding proteins using western blotting: use of the method for dissection of the binding junctions and competitor binding studies. *Anal Biochem* 154:138-143
- Zupi J, Sun W, Chang JV, James P, Proesch CR, Fischer JA 1990 Isolation and N-terminal amino acid sequences of rat serum carrier proteins for insulin-like growth factor. *Stability*. *Mophys Rev Commun* 36:118-1191
- How V, Oh Y, Rosenfeld KG 1996 Insulin-like growth factor-binding protein: a proposed superfamily. *Acta Endocrinol Suppl* 43:47-49
- Baker RC, Bennis M, Clemons DR, Chinnery C, Drap AIA, Holly JMP, Mohan S, Oh Y, Rosenfeld RG 1990 Recommendations for nomenclature for the insulin-like growth factor binding protein (IGFBP) superfamily. *J Clin Endocrinol Metab* 83:3213
- How V, Oh Y, Rosenfeld RG, The insulin-like factor binding protein (IGFBP) superfamily. *Endocr Rev* 1996
- Collett-Balding M, Cohen P 1996 The role of the insulin-like growth factor binding proteins and the IGFBP protease in modulating KTF action. *Endocrinol Metab Clin North Am* 25:601-614
- Chung PT, Wu J, Bansal W, Chinenawuk SI 1994 Characteristic regulation of an insulin-like growth factor-binding protein-4 peptide produced by a rat neuronal cell line. *Endocrinology* 135:1328-1335
- Chenauwa B, Smith CL, Dutton KL, Husby WH, Wright C, Clemons DK 1994 Proteolytic cleavage of insulin-like growth factor binding protein 4 (IGFBP-4). Identification of cleavage site in amide-terminal region of native IGFBP-4. *J Biol Chem* 271:11377-11382
- Andress UL, Wienbaum M 1992 Human osteoblast derived insulin-like growth factor (IGF) binding protein-5 stimulates osteoblast mitogenesis and potentiates KTF action. *J Biol Chem* 267:29463-29477
- Andress UL, Logel SM, Zapf J, Koeffler MC 1993 Carboxy-truncated insulin-like growth factor binding protein-5 stimulates mitogenesis in osteoblast like cells. *Biotech Biophys Rev Commun* 16(6):40
- Oh Y, Strong DM, Rayfield DJ, Mohan S 1994 Structure-function analysis of the human insulin-like growth factor binding protein. *J Biol Chem* 273:23509-23516
- Brinkman A, Grotten CA, Kortleve DJ, Kessel AGV, Drap SL 1990 Isolation and characterization of a cDNA encoding the low molecular weight insulin-like growth factor binding protein (IGFBP-1). *EMBO J* 9:411-418
- Oh Y, Strong DM, Rayfield DJ, Mohan S 1994 Structural determinants of ligand and cell surface binding of insulin-like growth factor-binding protein-1. *J Biol Chem* 273:2301-2309
- Beurne U, Beurne U 1994 Characterization of glycosaminoglycan binding domains in insulin-like growth factor-binding protein-3. *J Biol Chem* 271:14607-14679
- Brennan S, Song JL, Beutle J, Tonner L, Flatt DJ, Allan GI 1999 Amino acids within the extracellular matrix (ECM) binding region (aa 112-212) of rat insulin-like growth factor binding protein (IGFBP-5) are important determinants in binding KTF. *J Mol Endocrinol* 21:117-124
- Devi GR, Day JC, Shultz DL, McDonald RG 1998 An insulin-like growth factor II (IGF-II) affinity-enhancing domain localized within extracytoplasmic repeat 13 of the K-ras G-mutant 6-phosphate receptor. *Mol Endocrinol* 11:1661-1673
- Schmidt N, Ronne E, Dano K 1996 Docosan interplay in the uridine receptor. Requirement for the third domain in high-affinity ligand binding and generation of ligand coated sites in distinct receptor domains. *J Biol Chem* 271:22885-22891
- de Vos AM, Ulrich M, Kosselkoff AA 1992 Human growth hormone and insulin-like domain of its receptor: crystal structure of the complex. *Science* 255:306-312
- Calmore AP, Wood L, Ohanian V, Jackson P, Patel B, Rees DJ, Hyneko RD, Critchley DE 1993 The cytoskeletal protein tail contains at least two distinct zinc binding domains. *J Cell Biol* 122:857-867
- Lenarcic B, Turc V 1997 Thyroglobulin-type-I domains in equine lactotrophin/pituitary lactotrophin/prolactin and cathepsin D. *J Biol Chem* 272:2564-2568
- Fowler JL, Thrall KJ, George-Nascimento C, Rosenberg CK, Bent DM 1997 Heparin-binding, highly basic regions within the thyroglobulin-type-I domain of insulin-like growth factor (IGF)-binding protein-1 (IGFBP-1), -3, -5, and -6 inhibit IGFBP-4 degradation. *Endocrinology* 138:2280-2287

Org. Op.	OPERATOR:	Session	PROOF:	PE's	AA's	COMMENTS	ARTNO:
1st disk, 2nd RWS	Jaffer S	5	/	/	/		868069

# **Cellular Expression of Insulin-like Growth Factor Binding Protein-3 Arrests the Cell Cycle and Induces Apoptosis in MCF-7 Human Breast Cancer Cells**

**Ho-Seong Kim, Angela R Ingermann, Junko Tsubaki, Stephen M Twigg and Youngman Oh**

*Department of Pediatrics, Oregon Health Sciences University, Portland, Oregon*

Running Title: IGFBP-3 arrests cell cycle and induces apoptosis

Address correspondence to :      Youngman Oh, Ph.D.,  
Associate Professor  
Department of Pediatrics  
Oregon Health Sciences University  
3181 S.W. Sam Jackson Park Road, NRC-5  
Portland, OR 97201-3098  
Tel: 503-494-1930  
Fax: 503-494-0428  
Email: ohy@ohsu.edu

**Summary:**

The IGFBPs are classically known to bind IGFs and modulate the IGF signaling system, however, emerging data have suggested that IGFBPs may play more active, IGF-independent roles in growth regulation in various cell systems. In support of this hypothesis, IGFBPs, in particular IGFBP-3, have been recently shown to potently inhibit proliferation of various cell types in an IGF-independent manner. However, the specific mechanism for the IGF-independent action of IGFBP-3 is not yet clearly understood. In the present study, we have demonstrated a novel, IGF-independent role for IGFBP-3; cell cycle arrest and induction of apoptosis in MCF-7 human breast cancer cells. MCF-7 cells, which do not produce IGF peptides, were stably transfected with an IGFBP-3 cDNA construct using the ecdysone-inducible expression system. Dose-dependent inducible production of IGFBP-3 protein was detected in the induced stably-transfected cells, compared to undetectable levels in control parental and uninduced stably-transfected cells. Induction of IGFBP-3 in these cells showed dose-dependent inhibition of DNA synthesis as assessed by [<sup>3</sup>H]-thymidine incorporation assays. This inhibitory effect was abolished by co-treatment with Y60L-IGF-I, an IGF analog which has significantly reduced affinity for the IGF receptor but retains high affinity for IGFBP-3, demonstrating specificity and IGF-independence. In addition, flow cytometry analysis showed that induced expression of IGFBP-3 led to an arrest of the cell cycle in G1-S phase. Induction of IGFBP-3 resulted in a significant decrease in the mRNA and protein levels of cyclin D, but not cyclin E, as well as concomitant decreases in the levels of cdk4, total-Rb, and phosphorylated-Rb, consistent with and presenting a possible mechanism for IGFBP-3-induced cell cycle arrest. Moreover, IGFBP-3 inhibited oncogenic Ras-induced phosphorylation of MAPKs, presenting the evidence for cross-talk of IGFBP-3 signaling with MAPK signal transduction pathway. IGFBP-3-expressing cells also displayed increased Annexin V binding compared to controls, exhibiting the IGFBP-3-induced apoptosis. Further studies demonstrated that IGFBP-3 caused an increase in caspase activities, suggesting a potential mechanism for the IGFBP-3-induced apoptosis. Taken together, present study shows that cellular production of IGFBP-3 leads to cell cycle arrest and induction of apoptosis, thereby inhibiting cell proliferation in these MCF-7 human breast cancer cells and suggesting that IGFBP-3 functions as a negative regulator of breast cancer cell growth, independent of the IGF axis.

**Key Words**

IGFBP-3, inducible stable cell line, cell cycle arrest, apoptosis, breast cancer, cyclin D1, retinoblastoma protein, caspase

## **Introduction:**

The insulin-like growth factor binding proteins (IGFBPs) are components of the IGF signaling system, and their superfamily is comprised of six high affinity species (IGFBPs 1-6) and several low affinity binders (IGFBP-related proteins (IGFBP-rPs)) (1-5). The classical role of the IGFBPs involves IGF binding and modulation of IGF signaling, however, recent data suggest that some IGFBPs may play more active, IGF-independent roles in growth regulation in various cell systems (6-19). In particular, IGFBP-3 has been shown to potently inhibit proliferation of various cell types in an IGF-independent manner. This concept of IGF-independent action of IGFBP-3 is supported by demonstrations that (1) exogenous IGFBP-3 binds to specific proteins on cell surface and this interaction is strongly correlated with the ability of IGFBP-3 to inhibit cell growth (8, 9); (2) overexpression of a transfected human IGFBP-3 cDNA inhibits cell proliferation (10-12); (3) IGFBP-3 mediates transforming growth factor-b (TGF-b)- (13), retinoic acid- (14), antiestrogen- (15), vitamin D analogs- (16), and tumor necrosis factor-a (TNF-a)- (17) induced growth inhibition; (4) regulation of IGFBP-3 gene expression plays a role in signaling by p53, a potent tumor-suppressor protein (18); and (5) IGFBP-3 fragments inhibit the stimulation of DNA synthesis induced either by IGF-I or insulin (19). Recently, several reports have demonstrated that IGFBP-3 induces apoptosis in PC-3 prostate cancer (20) and MCF-7 breast cancer cells (21), and increases ceramide-induced apoptosis in Hs578T breast cancer cell line (22). However, the specific mechanism for the IGF-independent action of IGFBP-3 is yet to be elucidated. Moreover, applications of the purified IGFBP-3 from biological fluids and recombinant species have showed limitation for the biological studies due to concerns about the purity, bioactivity and post-translational modification of IGFBP-3. In this study, we have investigated a novel, IGF-independent role for IGFBP-3; cell cycle arrest and induction of apoptosis in MCF-7 human breast cancer cells by inducible cellular expression of IGFBP-3.

We hypothesized that IGFBP-3 inhibits cell growth in an IGF-independent manner and were interested to determine whether its growth-inhibitory effects involve regulation of the cell cycle arrest and/or induction of apoptosis. To address these questions, we generated a subline of MCF-7 cells (which do not produce IGF peptides) stably transfected with an inducible IGFBP-3 cDNA construct using the ecdysone-inducible expression system. This controlled system was used to look carefully at the effects of induced IGFBP-3 expression on the cell cycle and apoptosis. We then investigated possible mechanisms of growth inhibition and the signal transduction pathways involved in inhibitory actions of IGFBP-3.

## **Experimental Procedures**

### *Materials*

Cells were purchased from American Type Culture Collection (Rockville, MA). Tissue culture reagents and plastics were purchased from Mediatech (Hemdon, VA), Becton Dickinson (Franklin Lakes, NJ) and Nunc (Naperville, IL). Monoclonal antibodies against cyclin D1 were purchased from NeoMarkers (Fremont, CA), cyclin D3 from Calbiochem (Cambridge, MA), cyclins A, E and poly(ADP-ribose) polymerase (PARP) from Santa Cruz Biotechnology (Santa Cruz, CA), cyclin-dependent kinase (cdk) 4 from Transduction Laboratories (Lexington, KY). Polyclonal antibodies against retinoblastoma protein (Rb), phospho-Rb, p44/42 mitogen-activated protein kinase (MAPK), and phospho-p44/42 MAPK were purchased from New England Biolabs/Cell Signaling Technology (Beverly, MA). Monoclonal antibody against IGFBP-3 and a radioimmunoassay kit for IGFBP-3 were generously provided by Diagnostic Systems Laboratories (Webster, Tx). Recombinant human IGF-I analog, Y60L-IGF-I was the generous gift of Protagen Inc. (Mountainview, CA). DEVD-AMC and LEHD-AMC flourogenic caspase substrate peptides were purchased from Biomol (Plymouth Meeting, PA). The ecdysone-inducible expression system was from Invitrogen (Carlsbad, CA). Human cyclin D1 cDNA was purchased from American Type Culture Collection (Rockville, MA). A constitutively active Ras (RasV12) cDNA expression construct was the kind gift of Dr. Philip Stork, Vollum Institute, OHSU, (Portland, OR). DNA preparations were made using kits from Qiagen (Chatsworth, CA).

### *Generation of an MCF-7-derived Inducible IGFBP-3 Cell Line*

A cDNA encoding human IGFBP-3 was cloned into the pIND expression vector. This construct was cotransfected with pVgRXR (encoding a hybrid ecdysone / retinoid X receptor) into MCF-7 cells using FuGene 6 transfection reagent (Roche, Indianapolis, IN). Cells were split 48 h later to low density into selective medium containing G418 (800 µg/ml) and zeocin (100 µg/ml). After 14 days, isolated foci of selection-resistant cells were subcultured and expanded. To test for the proper inducible expression of IGFBP-3, each clone was cultured in the presence of the inducer ponasterone A (2-15 µM). Conditioned media (CM) were collected to test for ponasterone-inducible expression of IGFBP-3 by western immunoblot. Hybrid receptor only-transfected (MCF-7:EcR) cells were used as a negative control.

### *Cell Cultures*

All cells were maintained in Dulbecco's modified Eagle's medium (DMEM) supplemented with 4.5 g/liter glucose, 110 mg/liter sodium pyruvate, and 10% fetal bovine serum. Stably-transfected MCF-7:EcR cells were maintained in selective medium containing 100 µg/ml zeocin. Stably-transfected MCF-7:BP-3 cells were maintained in selective medium containing 800 µg/ml G418 and 100 µg/ml zeocin. For studies involving the induction of IGFBP-

3 expression, cells were seeded and cultured until 60–70% confluent, then switched to serum-free media with or without 15 μM ponasterone A for 72 h, unless otherwise indicated in the text. CM were collected and centrifuged at 1000 X g for 10 min to remove cell debris.

#### *[<sup>3</sup>H] Thymidine Incorporation Assay*

Cells were seeded and cultured in 24-well dishes. After three days of IGFBP-3 induction, a 4 h pulse of 0.1 μCi of [<sup>3</sup>H] thymidine (25 Ci/mM; NEN, Boston, MA) in a volume of 25 μl was added to each well. Cells were incubated, and the rate of DNA synthesis was estimated by measuring the trichloroacetic acid-precipitable radioactivity, as described previously (23).

#### *Flow Cytometry: Cell Cycle and Apoptosis Assays*

Cells were seeded and cultured in 6-well dishes, then induced to express IGFBP-3. Cells were harvested, pelleted at 1000 rpm for 5 min and washed three times with phosphate-buffered saline (PBS). For cell cycle analysis, each sample was resuspended in propidium staining solution (50 mg/ml propidium iodide, 100 U/ml RNase A, 0.1% Triton X-100, 0.1% sodium azide in PBS) and incubated for 30 min in the dark. Analysis of apoptotic cells was performed using FITC-conjugated Annexin V (Santa Cruz Biotechnology, Santa Cruz, CA) according to the manufacturer's directions. Data were collected on a FACSCalibur flow cytometer (Becton Dickinson, Franklin Lakes, NJ) equipped with an argon laser. The data were analyzed using Cell Quest software (Becton Dickinson).

#### *Western Immunoblotting*

Cell lysates were prepared as described previously with minor modifications (24). In brief, confluent cells were washed with cold PBS, then scraped from plates in the presence of cold RIPA lysis buffer containing 20 mM Tris, pH 8.0, 150 mM NaCl, 1% Nonidet P-40, 0.5% Na DOC, 0.1% SDS, containing a protease inhibitor cocktail (Roche, Indianapolis, IN). Cell lysates were rocked for 15 min at 4°C, then centrifuged to remove cell debris. The aliquots were stored at –70°C until use. Conditioned media samples were fractionated by 12% SDS-polyacrylamide gel electrophoresis (SDS-PAGE) under nonreducing conditions, while cell lysate samples were fractionated under reducing conditions. Fractionated proteins were electrotransferred onto Hybond-ECL nitrocellulose (Amersham Pharmacia, Arlington, VA). Membranes were blocked in 5% nonfat dry milk in Tris-buffered saline with 0.1% Tween-20 (TBST), and incubated with primary antibodies diluted in TBST for 2 h at room temperature or overnight at 4°C. Membranes were washed in TBST, then incubated with horseradish peroxidase-conjugated secondary antibodies (Southern Biotechnology Associates, Birmingham, AL), diluted 1:7000, for 1 h at room temperature. Immunoreactive proteins were detected using Renaissance Western Blot Chemiluminescence reagents (NEN, Boston, MA).

### *Northern Blot Analysis*

Total RNAs from monolayer cultures of IGFBP-3-transfected stable cell line cultured with or without ponasterone A were isolated using the RNeasy RNA isolation kit (Qiagen, Chatsworth, CA), and quantitated by absorbance at 260 nm. Five µg of total RNA were electrophoresed on 1% formaldehyde gels and transferred to GeneScreen Plus nylon membranes (NEN). Membranes were UV crosslinked and stained in 0.02% methylene blue / 0.3 M NaOAc, pH 5.5 to verify equivalent loading and transfer.  $^{32}$ P-labelled cDNA probes were prepared using the Prime It kit (Stratagene, Cedar Creek, TX). Membranes were hybridized in ULTRAhyb buffer (Ambion, Austin, TX) overnight at 42°C, and washed in 0.1 X SSC as described (3).

### *Densitometric and Statistical Analysis*

Densitometric measurement of immunoblots were performed using a Bio-Rad GS-670 Imaging densitometer (Bio-Rad, Melville, NY). All experiments were conducted at least three times. The data were analyzed with Student's *t* test, using the Microsoft Excel 98 software package.

### *Caspase Assay*

Cells were seeded in 96-well plates until 90% confluent, then incubated in triplicate with or without ponasterone A for the times indicated. Cells were lysed in 30 µl per well of ice-cold lysis buffer (50 mM HEPES, pH 7.4, 0.1% CHAPS, 0.1% Triton X-100, 1 mM DTT, 0.1 mM EDTA). 20 µl of each lysate was used in assays for caspase activity using a combination of two fluorogenic peptide substrates, DEVD-AMC and LEHD-AMC, which together cover specificity for a wide range of caspases. Lysates were distributed into a 96-well black plate and diluted in 190 µl of assay buffer (50 mM HEPES, pH 7.4, 100 mM NaCl, 0.1% CHAPS, 10 mM DTT, 1 mM EDTA, 10% glycerol). Serial dilutions of free 7-amino-4-methylcoumarin (AMC, Sigma, St. Louis, MO) diluted in assay buffer were included to generate a reference standard curve for determination of the amount of AMC released in each reaction. The plate was pre-incubated for 10 minutes at 37°C, then the reactions were started with the addition of DEVD-AMC and LEHD-AMC to each well to a final concentration of 40 µM each. Reaction kinetics were monitored for up to 16 hours at 37°C in a Bio-Rad Fluoromark fluorometer, with plate readings taken every 10 minutes at excitation/emission of 390nm/460nm. Of the remaining cell lysate, 5 ml were assayed for protein content. Data were analyzed from the linear portion of the reactions using Microplate Manager software (Bio-Rad), and final results were adjusted for protein content.

*Immunocytochemistry*

Cells were seeded in 8-chamber slides and cultured until 70% confluent, then incubated with or without ponasterone A for 48 or 72 hours. Cells were then rinsed twice in PBS, fixed in 4% paraformaldehyde, then rinsed again in PBS. For some antibodies, cells were additionally incubated in ice-cold methanol for 2 minutes on ice. Slides were blocked in 5% normal goat serum / PBS / 0.1% Triton for 1-2 hours at RT, then incubated with primary antibodies diluted in blocking solution at 4°C overnight. Slides were rinsed 3 times 5 minutes in PBS and incubated with secondary antibodies diluted in blocking solution for 1 hour at RT. Slides were rinsed as before, and cells were covered in 50% glycerol before coverslipping. Data were collected on a Nikon (Melville, NY) Diaphot 300 inverted fluorescent microscope equipped with a 1.3 megapixel CCD camera (Princeton Instruments, Trenton, NJ) using IPLab software (Scianalytics, Fairfax, VA).

## Results

### *Induced Expression of IGFBP-3 in the MCF-7-derived Stable Cell Lines*

For these studies we developed a subline of MCF-7 human breast cancer cells which expresses IGFBP-3 when cultured in medium containing an inducing compound, ponasterone A. The parental MCF-7 cells do not express detectable levels of IGFBP-3, and also do not express IGF peptides (25), making this cell line an ideal choice. A total of 16 selection-resistant clones were generated, and these were tested for inducible expression of IGFBP-3 by western immunoblotting of conditioned media (CM) samples. Figure 1 shows the panel of IGFBP-3 protein production from these 16 clones. IGFBP-3 was expressed in clones #2, #3, and #6 in an inducible manner, while constitutively expressed in clones #1 and #16. Expression of IGFBP-3 could be detected from 24 h at the concentrations of ponasterone A ranging from 1 to 15  $\mu$ M without affecting the cell viability (data not shown). Clone #3 (MCF-7:IGFBP-3 #3) was used for further experiments. Quantitative analysis of IGFBP-3 protein levels in CM of induced MCF-7:IGFBP-3 #3 cells using a radioimmunoassay indicated that maximal levels of IGFBP-3, ranging from approximately 100-150 ng/ml, occurs on day 3 at the concentration of 15  $\mu$ M ponasterone A.

### *IGF-independent Inhibition of DNA synthesis by IGFBP-3*

Induced expression of IGFBP-3 by ponasterone A resulted in an inhibition of DNA synthesis compared to IGFBP-3-uninduced cells (MCF-7:IGFBP-3 #3 without ponasterone A), shown in Fig. 2A. This inhibitory effect of IGFBP-3 was dose-dependent, with 45% inhibition at a concentration of 10  $\mu$ M ponasterone A ( $p<0.001$ ). Meanwhile, an inhibition of DNA synthesis in pVgRXR-transfected control cells (MCF-7:EcR) was not prominent. This effect of IGFBP-3 does not result from blocking the mitogenic actions of IGFs by preventing their binding to IGF receptors, because MCF-7 cells, which do not produce IGF peptides (25), were cultured in SFM in our system to exclude the effects of IGFs. Moreover, this IGFBP-3-induced inhibitory effect was abolished by co-treatment with Y60L-IGF-I, an IGF analog with a leucine for tyrosine substitution at amino acid position 60, has a 100-fold reduced affinity for IGF receptors but full affinity for IGFBP-3, demonstrating the specificity of the IGF/IGF receptor-independent action of IGFBP-3 (Fig. 2B).

### *IGFBP-3 Arrests the Cell Cycle and Regulates Cell Cycle-related Proteins*

To identify the mechanism for the growth-inhibitory effect of IGFBP-3, we performed flow cytometry analysis. MCF-7:IGFBP-3 #3 and EcR cells cultured in SFM with or without ponasterone A were used to analyze the cell cycle profile by propidium iodide staining of DNA content followed by flow cytometry detection. The treatment of MCF-7:IGFBP-3 #3 with 15  $\mu$ M ponasterone A caused a decrease in the percentage of cells in the S phase, from 18.4% in the absence of ponasterone A to 13.8% and an accumulation of cells in the G1 phase from 72.1% to 78.1% (Fig. 3). There was no

change in the cell cycle distribution in EcR cells treated with ponasterone A (data not shown). These results suggest that induced expression of IGFBP-3 leads to a cell cycle arrest in the G1/S phase. We further examined whether IGFBP-3 affects the levels of cell cycle regulatory proteins, such as cyclin D1, cyclin D3, cyclin A, cdk4, Rb, and phospho-Rb, which are known as key cell cycle regulatory proteins for progression through G1 phase of the cell cycle in breast epithelial cells (27, 28). Firstly, we examined steady-stable cyclin D1 mRNA level by northern blotting using MCF-7:IGFBP-3 #3 cells cultured in SFM with or without ponasterone A (Fig. 4A). Both cyclin D1 mRNA species, approximately 4.5 and 1.5 kb in size, were observed in MCF-7:IGFBP-3 #3 cells. A significant decline in 4.5 kb cyclin D1 mRNA levels were observed from 24 h after addition of ponasterone A. In contrast, the 1.5 kb mRNA species was not affected by addition of ponasterone A. The expression of IGFBP-3 mRNA was observed from 12 h, before the decrease in expression of cyclin D1 mRNA. Hybridization with b-actin showed equal loading of the gel. Further, immunoblot analysis revealed a concomitant decline in the levels of cyclin D1 protein (Fig. 4B). Addition of ponasterone A resulted in a reduction in cyclin D1 in MCF-7:IGFBP-3 #3 cells, but not in EcR cells. Decreased levels of cyclin D1 in MCF-7:IGFBP-3 #3 cells with ponasterone A was reversed by co-treatment of Y60L-IGF-I (Fig. 4C), suggesting the IGFBP-3 either directly or indirectly is involved in regulating cyclin D1 expression in an IGF/IGF receptor-independent manner.

Further analysis of various cell cycle-regulated proteins was performed in MCF-7:IGFBP-3 #3 cells cultured in SFM with or without ponasterone A at 0, 24, 48, 72 h. As shown in Fig. 5A, the levels of cyclin D1, cdk4, total Rb, and phosphorylated Rb were decreased from day 1 and levels of cyclin A from day 3, while the levels of cyclins D3 and E were unchanged. These results suggest that IGFBP-3 specifically decreases the levels of cyclin D1, cdk4, and total and phosphorylated Rb in these cells, presenting a possible mechanism for IGFBP-3-induced cell cycle arrest in G1/S phase. Ultimately, the decreased levels of Rb and phosphorylated Rb may serve to directly suppress exit from G1 phase. Additionally, as shown in Fig 5B, immunocytochemistry experiments revealed a similar pattern of decreased protein levels. Immunodetectable levels of Cyclin D1 and phosphorylated Rb proteins were significantly reduced in cells induced to express IGFBP-3 compared to controls.

#### *Effect of IGFBP-3 on the MAPK signaling pathway*

Previous studies indicated that mitogen-activated protein kinase (MAPK) cascades modulate the expression of cyclin D1 (29), thus we examined the effect of IGFBP-3 on MAPK cascade proteins. Fig. 6A shows that the levels of phosphorylated, but not total p44/42 MAPK was decreased in MCF-7:IGFBP-3 #3 cells after induction of IGFBP-3 with ponasterone A. Further, immunofluorescent microscopy studies demonstrated that induced expression of IGFBP-3 results in significant decrease as well as disturbed subcellular localization of phosphorylated p44/42 MAPK (Fig. 6B). This suggests that the IGFBP-3-mediated decrease in cyclin D1 results, at least in part, of modulation of p44/42

MAPK activity.

To further investigate the cross-talk between IGFBP-3 signaling and the MAPK signaling cascades, we transiently transfected constitutively active Ras (RasV12) into our cell system. As shown in Fig. 7, overexpression of oncogenic Ras resulted in stimulation of DNA synthesis as well as activation of p44/42 MAPK. Induction of IGFBP-3 expression caused a significant inhibition of both oncogenic Ras-induced DNA synthesis and p44/42 MAPK phosphorylation. Taken together, these data suggest that IGFBP-3 antagonizes Ras-MAPK signaling cascades.

*IGFBP-3 induces apoptosis*

At the same time, we determined whether IGFBP-3 could induce apoptosis using the annexin V binding assay, which is used to identify cells in the early stages of the apoptotic process (26). Fig. 8A shows that induced expression of IGFBP-3 caused increase in the percentage of cells in the apoptosis, from 1.5% in the absence of ponasterone A to 36%, suggesting that IGFBP-3 induces apoptosis in this cell system. Additional indication that IGFBP-3 induces apoptosis came from results of assays for caspase activity. The data in Fig 8B demonstrate that induction of IGFBP-3 expression causes an increase caspase activity in these cells as measured by incubating cell lysates with a combination of the purified fluorogenic caspase substrate peptides DEVD-AMC and LEHD-AMC. Caspase activity in uninduced cells lysates was detected at an average of 7.8 pmol AMC released/min/mg to an average of 10 pmol/min/mg with induced IGFBP-3 expression ( $p < 0.05$ ) at 48 hrs. In addition, IGFBP-3 increases caspase activity in a dose-dependent manner. The topoisomerase II inhibitor etoposide, and taxol, which reversibly binds to tubulin, were used as control apoptosis inducers. To present further evidence of capase activation by IGFBP-3, we examined cleavage of one caspase substrate, poly(ADP-ribose) polymerase (PARP) by immunoblotting. This nuclear enzyme is proteolytically cleaved by activated caspases during apoptosis (30). As shown in Fig. 8C, the induced expression of IGFBP-3 resulted in an increase of the 85 kDa carboxy terminal fragment of PARP, confirming that IGFBP-3 induces apoptosis at least, in part, through activation of caspases in MCF-7 breast cancer cell system.

## **Discussion**

A growing accumulation of data has demonstrated that some IGFBPs, including IGFBPs -1, -3, -5, and presumably IGFBP-rPs, have their own IGF-independent biological actions (3, 5, 8-11). In particular, the IGF-independent effects of IGFBP-3 have been reported in various cell systems by treatment of recombinant IGFBP-3 exogeneously or use of stable transfection systems. However, its action requires relatively high concentrations of recombinant IGFBP-3, ranging 500-1500 ng/ml to achieve biological effects of IGFBP-3 (8, 11, 20, 21). At present study, we utilize the ecdysone-inducible expression system in MCF-7 human breast cancer cells, and thereby examining the biological effects of endogenous IGFBP-3 expressed under controlled induction. As demonstrated, human endogenous IGFBP-3 was induced ranging 100-150 ng/ml in our cell system, of which concentrations appear to be comparable to those obtained in conditioned media after treatment of various reagents, such as TGF- $\beta$ , RA, TNF- $\alpha$  and antiestrogen, for investigation of biological function of induced IGFBP-3 in various cell systems. Our results demonstrate that this lower concentration of endogenous IGFBP-3 is sufficient to inhibit DNA synthesis and induces apoptosis, despite relatively high concentrations (300-1000 ng/ml) of recombinant IGFBP-3 which were required to obtain similar biological effects of IGFBP-3 in MCF-7 cells (21). It is tempting to speculate that difference in the sensitivity of IGFBP-3 on biological function may result from the difference of IGFBP-3 preparations, that is a natural vs. recombinant form, and endogenous secretory protein from the cell or exogenous form added to the cultures. In addition, post-translational modifications, such as glycosylation and phosphorylation, may affect the sensitivity. On the other hand, sensitivity to IGFBP-3 may determine whether the cell types express the oncogenes or other molecules which influence the signaling pathways in the development of IGFBP-3 insensitivity. Martin and Baxter (31) reported that resistance to IGFBP-3 is induced in normal mammary epithelial cells transfected with oncogenic ras, thereby activating the MAPK/ERK pathway. In contrast, MCF-10A normal human mammary epithelial cells, which require 10-100 ng/ml human plasma-derived IGFBP-3 to achieve a similar level of inhibition to that seen with 500-1500 ng/ml in the transformed cells, are considerably more sensitive to IGFBP-3 than breast cancer cells. Increased activity of oncogenic Ras-dependent signaling pathways is implicated in the development of IGFBP-3 insensitivity (31). It is of note that MCF-7 cells do not express oncogenic Ras, which may explain why such low concentrations of IGFBP-3 are sufficient to exert its biological effects.

The IGF-independent effect of IGFBP-3 has been extensively investigated in variety of cell systems, however, the mechanisms by which these actions are exerted are not fully elucidated. Recent studies have proposed that IGFBP-3 functions as an apoptosis-inducing agent and that this action is mediated through a p53- and IGF-independent pathway in PC-3 prostate cancer cells (20), whereas IGFBP-3 has no direct inhibitory effect on Hs578T breast cancer cells but could accentuate apoptosis induced by ceramide (22). On the other hand, a vitamin D3 analog (Ro 24-5531) inhibits cell growth and increases the IGFBP-3 mRNA and protein levels in human osteosarcoma cell line, and the

inhibition in cell growth is accompanied by a decrease in the expression of p34cdc2, a protein critically involved in cell cycle regulation. These studies have provided circumstantial evidence that IGFBP-3 involves cell growth arrest (32). Our present studies focus on identification of the potential mechanism for IGFBP-3-induced growth inhibition, and demonstrate for the first time that IGFBP-3 induces cell cycle arrest in G1 phase by regulating expression of cell cycle-regulatory proteins, in particular cyclin D1, as well as inducing apoptosis by modulating proapoptotic caspase activities.

Since IGFBP-3 prevents cell cycle progression at G1 phase, we determined whether IGFBP-3 affects cell cycle-regulated proteins in MCF-7:IGFBP-3 #3 cells. Components responsible for the coordinated progression through the cell cycle include the cyclin-dependent kinases (cdks), regulatory cyclin subunit, and cdk inhibitors (33-35). Once extracellular signals activate the synthesis of the regulatory cyclin subunit, appropriate sites on the catalytic subunit must be phosphorylated by the cdk-activating kinase (CAK, also known cdk7) to phosphorylate the product of the Rb gene, resulting in the derepression of E2F/DP-dependent transcription and passage through S phase of the cell cycle (36, 37). D-type cyclins (cyclins D1, D2, and D3), in conjunction with their catalytic partners, cdk4 and cdk6, have been known to execute their critical functions during mid-to-late G1 phase, as cells cross a G1 restriction point (33). Overexpression of cyclin D1 can shorten the G1 cell cycle phase, decrease cell size, reduce requirements for growth factors (38-40). Microinjection of antisense constructs or antibodies to cyclin D1 into normal fibroblasts can prevent them from entering S phase (38, 41). In contrast, cyclin E is expressed later in G1 phase and its expression is periodic and maximal at the G1-S transition (42). In our study, we have found that induction of IGFBP-3 leads to inhibition of expression of cyclin D1 mRNA followed by a reduction in protein levels, and concomitant decrease of cdk4, total Rb, and phospho-Rb proteins, indicating a possible mechanism of cell cycle arrest in G1/S phase. In contrast, cyclin D3, cyclin A, and cyclin E do not show any change, suggesting that cyclin D1 is a major player in the regulation of G1-S phase progression by IGFBP-3 in MCF-7 cells. Cyclin D1 is important for neoplastic transformation as well as cell cycle pregression. When cyclin D1 is cotransfected with other oncogenes, such as activated Ha-ras or adenovirus E1A into human fibroblast, malignant transformation of cells has been reported (43, 44). Overexpression of cyclin D1 in the mammary gland of transgenic mice induces mammary carcinoma (45). Moreover, dysregulated cyclin D1 expression have been observed in human neoplasia, including breast cancer (46, 47). These results suggest that IGFBP-3, which is able to modulate cyclin D1 expression, has a potential role in a strategy for anti-cancer therapy.

The expression of cyclin D1 is known to be regulated by transcriptional, translational, and posttranscriptional processes (48, 49). Multiple signaling pathways seem to be involved in the regulation of cyclin D1 expression at a transcriptional level. Previous studies have shown that cyclin D1 expression is regulated by the p42/p44 MAPK, p38 MAPK, and Jun kinases (JNKs) (29). Moreover, direct induction of cyclin D1 can be achieved by serum, growth factors, cytokines, Rb, oncogenic Ras, and Src kinase (29, 50-53). Ectopic expression of E2F1 inhibits the cyclin D1

protein at the transcriptional level, suggesting a negative feedback for cells already in S phase (54). Decreased expression of cyclin D1 by IGFBP-3 shown in this study may be, at least in part, associated with the decreased level of p42/p44 MAPK activity. Our results demonstrated that induced expression of IGFBP-3 results in inhibition of not only basal level of phosphorylation of p42/p44 MAPK but also oncogenic-Ras-induced phosphorylation of p42/p44 MAPK, indicating that IGFBP-3 appears to interact with the Ras-MAPK signaling cascades, presumably on a downstream effector of Ras and thereby regulating cyclin D1 expression and subsequent cell cycle progression. More proximal events of IGFBP-3-induced antagonism of the MAPK signaling pathway will be the subject of future studies in our laboratory.

Beyond arrest of the cell cycle, our data also indicate that cellular expression of IGFBP-3 promotes apoptosis in MCF-7 cells. Apoptosis is a major multi-faceted form of cell death, that has been implicated as playing a role in several human diseases, including cancer. There are a series of events involved in the commitment and execution of apoptotic cell death, several of which have been well characterized. Among these are changes in the plasma membrane, with the enzymatically-driven translocation or "flipping" of phosphatidylserine (PS) to the extracellular surface. The result of this process can be detected utilizing the binding properties of Annexin V, which binds preferentially to PS and other negatively charged phospholipids. Our results show a clear and significant increase in annexin V binding in cells induced for IGFBP-3 expression relative to controls. Another indicator of the apoptotic process is caspase activity. Caspases are a family of evolutionarily related cysteine-dependent proteases, with an universal specificity for Asp in the P<sub>1</sub> position, that play a prominent role during the progression of apoptosis. Activation of caspases and subsequent cleavage of critical cellular substrates are implicated in many of the morphological and biochemical changes associated with apoptotic cell death. Using an assay which detects activity of a broad range of caspases, we demonstrate a measurable and reproducible increase in caspase activity in IGFBP-3-induced cells relative to control uninduced cells, and further the increase in caspase activity was dose-dependent with regard to IGFBP-3. Furthermore, increased cleavage of the caspase substrate poly(ADP-ribose) polymerase (PARP) was observed after induction of IGFBP-3 expression. The nuclear enzyme PARP is proteolytically cleaved by activated caspases, primarily caspases 3 and 7 during apoptosis, but can also be cleaved in vitro by a wide range of caspases (30). It is of note that MCF-7 cells do not express caspase 3 due to a functional deletion of the gene (55), suggesting that the IGFBP-3-induced activation of caspase activity may be mediated primarily through caspase 7 and others. Nevertheless, these three lines of evidence indicate that induction / promotion of apoptosis is a major effect of cellular expression of IGFBP-3 in these cells.

Our previous studies have demonstrated that IGFBP-3 inhibits cell growth in an IGF-independent manner through an IGFBP-3 receptor in Hs578T breast cancer cells (8, 9, 13). In addition, we have sequenced and characterized a novel gene/protein which specifically interacts with IGFBP-3, designated IGFBP-3 receptor (BP3-R) (unpublished data). When we transfected BP3-R into IGFBP-3-induced cells, DNA synthesis was further inhibited (by an aver-

age of 65%) compared to control IGFBP-3-induced cells (an average of 45%), suggesting that IGFBP-3 and BP-3R appear to cooperatively suppress DNA synthesis and cell growth, to an extent greater than that seen with IGFBP-3 alone (unpublished data). Furthermore, BP-3 R alone without induction of IGFBP-3 results in no significant changes in DNA synthesis and cell growth in the same cell system, suggesting necessity of interaction between IGFBP-3 and BP-3R for IGFBP-3-induced biological function.

We thus concluded that cellular expression of IGFBP-3 inhibits DNA synthesis and cell growth through the cell cycle arrest in G1 phase and induction of apoptosis at physiological concentrations in an IGF-independent manner in MCF-7 breast cancer cells. Regardless of the underlying mechanisms, the present study demonstrates that IGFBP-3 decreases the levels of cyclin D1 protein, followed by cdk4, Rb, and phospho-Rb, indicating a possible mechanism of cell cycle arrest. Although we cannot exclude a possible additional posttranscriptional and translational regulation of cyclin D1 by IGFBP-3, our results suggest that IGFBP-3 decreases the cyclin D1 expression at the level of transcription, in part, through the decline in p42/p44 MAPK expression. This novel cell cycle regulatory and apoptosis-inducing aspect of IGFBP-3 have clinical significance in the prevention and/or treatment of human neoplasia, particularly in conjunction with IGFBP-3 receptor.

## References

1. Shimasaki, S., and Ling, N. (1991) *Progress Growth Factor Res.* **3**, 243-266
2. Jones, J. I., and Clemmons, D. R. (1995) *Endocr. Rev.* **16**, 3-34
3. Kim, H. -S., Nagalla, S. R., Oh, Y., Wilson, E., Roberts, C. T. Jr., and Rosenfeld, R. G. (1997) *Proc. Natl. Acad. Sci. U. S. A.* **94**, 12981-12986
4. Baxter, R. C., Binoux, M.A., Clemmons, D. R., Conover, C. A., Drop, S. L. S., Holly, J. M. P., Mohan, S., Oh, Y., and Rosenfeld, R. G. (1998) *Endocrinology* **139**, 4036
5. Hwa, V., Oh, Y., and Rosenfeld, R. G. (1999) *Endocr. Rev.* **20**, 761-787
6. Villaudy, J., Delbe, J., Blat, C., Desauty, G., Golde, A., and Harel, L. (1991) *J. Cell Physiol.* **149**, 492-496
7. Liu, L., Delbe, J., Blat, C., Zapf, J., and Harel, L. (1992) *J. Cell. Biol.* **153**, 15-21
8. Oh, Y., Muller, H.L., Lamson, G., and Rosenfeld, R. G. (1993) *J. Biol. Chem.* **268**, 14964-14971
9. Oh, Y., Muller, H. L., Pham, H. M., and Rosenfeld, R. G. (1993) *J. Biol. Chem.* **268**, 26045-26048
10. Cohen, P., Lamson, G., Okajima, T., and Rosenfeld, R. G. (1993) *Mol. Endocrinol.* **7**, 380-386
11. Valentinis, B., Bhala, A., De Angelis, T., Baserga, R., and Cohen, P. (1995) *Mol. Endocrinol.* **9**, 361-367
12. MacDonald, R. G., Schaffer, B. S., Kang, I.-J., Hong, S. M., Kim, E. J., and Park J. H. Y. (1999) *J. Gastroenterol. Hepatol.* **14**, 72-78
13. Oh, Y., Muller, H. L., Ng, L., and Rosenfeld, R. G. (1995) *J. Biol. Chem.* **270**, 13589-13592
14. Gucev, Z. S., Oh, Y., Kelly, K. M., and Rosenfeld, R. G. (1996) *Cancer Res.* **56**, 1545-1550
15. Huynh, H., ang, X., and Pollak, M. (1996) *J. Biol. Chem.* **271**, 1016-1021
16. Colston, K. W., Perks, C. M., Xie, S. P., and Holly, J. M. (1998) *J. Mol. Endocrinol.* **20**, 157-162
17. Rozen, F., Zhang, J., and Pollak, M. (1998) *Int. J. Oncol.* **13**, 865-869
18. Buckbinder, L., Talbott, R., Velasco-Miguel, S., Takenata, I., Faha, B., Seizinger, B. R., and Kley, N. (1995) *Nature* **377**, 646-649
19. Lalou, C., Lassarre, C., and Binoux, M. (1996) *Endocrinology* **137**, 3206-3212
20. Rajah, R., Valentinis, B., and Cohen P. (1997) *J. Biol. Chem.* **272**, 12181-12188
21. Nickerson, T., Huynh, H., and Pollak, M. (1997) *Biochem. Biophys. Res. Commun.* **237**, 690-693
22. Gill, Z. P., Perks, C. M., Newcomb, P. V., and Holly, J. M. P. (1997) *J. Biol. Chem.* **272**, 25602-25607
23. Beukers, M. W., Oh, Y., Zhang, H., Ling, N., and Rosenfeld, R. G. (1991) *Endocrinology* **128**, 1201-1203
24. Sakaguchi, K., Yanagishita, M., Takeuchi, Y., and Aurbach, G. D. (1991) *J. Biol. Chem.* **266**, 7270-7278
25. Gebauer, G., Jager, W., and Lang, N. (1998) *Antican. Res.* **18**, 1191-1195
26. Chan, A., Relter, R., Wiese, S., Fertig, G., and Gold, R. (1998) *Histochem. Cell. Biol.* **110**, 553-558
27. Sherr, C. J. (1996) *Science*, **274**, 1672-1677
28. Sweeney, K. J., Musgrove, E. A., Watts, C. K., and Surherland, R. L. (1996) *Cancer Treat Res.* **83**, 141-170
29. Albanese, C., Johnson, J., Watanabe, G., Eklund, N., Vu, D., Arnold, A., and Pestell, R. G. (1995) *J. Biol. Chem.* **270**, 23589-23597
30. Fernandes-Alnemri, T., Takahashi, A., Armstrong, R., Krebs, J., Fritz, L., Tomaselli, K. J., Wang, L., Yu, Z., Croce, C. M., Salvenson, G., Earnshaw, W. C., Litwack, G., and Alnemri, E. S. (1995) *Cancer Res.* **55**, 6045-6052.

31. Martin, J. L., and Baxter, R. C. (1999) *J. Biol. Chem.* **274**, 16407-16411
32. Velez-Yanguas, M. C., Kalebic, T., Maggi, M., Kappel, C. C., Letterio, J., Uskokovic, M., and Helman, L. J. (1996) *J. Clin. Endocrinol. Metab.* **81**, 93-99
33. Sherr, C. J. (1993) *Cell* **73**, 1059-1065
34. Morgan, D. O. (1997) *Annu. Rev. Cell Dev. Biol.* **13**, 261-291
35. Reed, S. I. (1997) *Cancer Surv.* **29**, 7-23
36. Weinberg, R. A. (1995) *Cell* **81**, 323-330
37. Dyson, N. (1998) *Genes Dev.* **12**, 2245-2262
38. Quelle, D. E., Ashmun, R. A., Shurtleff, S.A., Kato, J. Y., Bar-Sagi, D., Roussel, M. F., and Sherr, C. J. (1993) *Genes Dev.* **7**, 1559-1571
39. Resnitzky, D., Gossen, M., Bujard, H., and Reed, S. I. (1994) *Mol. Cell. Biol.* **14**, 1669-1679
40. Imoto, M., Doki, Y., Jian, W., Han, E. K., and Weinstein, I. B. (1997) *Exp. Cell Res.* **236**, 173-180
41. Tam, S. W., Theodoras, A. M., Shay, J. W., Draetta, G. F., and Pagano, M. (1994) *Oncogene* **9**, 2663-2674
42. Dulic, V., Lees, E., and Reed, S. I. (1992) *Science* **257**, 1958-1961
43. Lovec, H., Sewing, A., Lucibello, F. C., Muller, R., and Moray, T. (1994) *Oncogene* **9**, 323-326
44. Hinds, P. W., Dowdy, S. F., Eaton, E. N., Arnold, A., and Weinberg, R. A. (1994) *Proc. Natl. Acad. Sci. U. S. A.* **91**, 709-713
45. Wang, T. C., Cardiff, R. D., Zukerberg, L., Lees, E., Arnold, A., and Schmidt, E. V. (1994) *Nature (Lond.)* **369**, 669-671
46. Buckley, M. F., Sweeney, K. J., Hamilton, J. A., Sini, R. L., Manning, D. L., Nicholson, R. I., deFazio, A., Watts, C. K., Musgrove, E. A., and Sutherland, R. L. (1993) *Oncogene* **8**, 2127-2133
47. Bartkova, J., Lukas, J., Muller, H., Strauss, M., Gusterson, B., and Bartek, J. (1995) *Cancer Res.* **55**, 949-956
48. Choi, Y. H., Lee, S. J., Nguyen, P., Jang, J. S., Lee, J., Wu, M. L., Taqkano, E., Maki, M., Henkart, P. A., and Trepel, J. B. (1997) *J. Biol. Chem.* **272**, 28479-28484
49. Sherr, C. J. (1995) *Trends Biochem. Sci.* **20**, 187-190
50. Westwick, J. K., Lambert, Q. T., Clark, G. J., Symons, M., Van Aelst, L., Pestell, R. G., and Der, C. J. (1997) *Mol. Cell. Biol.* **17**, 1324-1335
51. Lee, R. J., Albanese, C., Stenger, R., Watanabe, G., Inghirami, G., Haines, G. K., Penar, P., Webster, M., Muller, W. J., Brugge, J., Davis, R., and Pestell, R. G. (1999) *J. Biol. Chem.* **274**, 7341-7350
52. Brown, J. R., Nigh, E., Lee, R. J., Ye, H., Thompson, M. A., Saudou, F., Pestell, R. G., and Greenberg, M. E. (1998) *Mol. Cell. Biol.* **18**, 5609-5619
53. Muller, H., Lukas, J., Schneider, A., Warthoe, P., Bartek, J., Eilers, M., and Strauss, M. (1994) *Proc. Natl. Acad. Sci. U. S. A.* **91**, 2945-2949
54. Watanabe, G., Albanese, C., Lee, R. J., Reutens, A., Vairo, G., Henglein, B., and Pestell, R. G. (1998) *Mol. Cell. Biol.* **18**, 3212-3222
55. Kirsch, D., Doseff, A., Chau B. N, Lim D. S., de Souza-Pinto, N. C., Hansford R., Kastan, M. B., Lazebnik Y. A., and Hardwick, J. M. (1999) *J. Biol. Chem.* **274**, 21155-21161.

**Fig. 1.** Panel of IGFBP-3 expression in 16 clones tested for induction with ponasterone A. MCF-7 cells were stably transfected using the ecdyson-inducible system. Transfected cells were selected in G418- and Zeocin-containing medium. Incubation of the cells with Ponasterone A induces the expression of IGFBP-3. Clones 1 and 16 constitutively expressed IGFBP-3; clones 2, 3, and 6 expressed IGFBP-3 in an inducible manner.

**Fig. 2.** Inhibitory effect of IGFBP-3 on DNA synthesis in inducible stably transfected MCF-7 cells. A) Cells were treated with ponasterone A at concentrations of 0-10  $\mu$ M for 72 h in SFM prior to assessing DNA synthesis by [<sup>3</sup>H]-thymidine incorporation. Significant decreases in DNA synthesis compared with noninducible control (receptor only) transfected cells were seen. B) Cells were treated with Y60L-IGF-I (100 ng/ml), an IGF-I analog with significantly reduced affinity for the IGF receptor but high affinity for IGFBPs, in the presence or absence of ponasterone A (10  $\mu$ M) as indicated for 72 h prior to assay for [<sup>3</sup>H]-thymidine incorporation. The inhibitory effect of IGFBP-3 was abolished by Y60L-IGF-I, demonstrating IGFBP-3 specificity and IGF-independency. \* = p<0.05, \*\* = p<0.001.

**Fig. 3.** Cell cycle arrest in the IGFBP-3-induced cells. Asynchronous MCF-7:IGFBP-3 #3 cells were seeded with or without ponasterone A in SFM for 72 h. The percentages of cells in the various phases of the cell cycle were determined by propidium iodide staining for DNA content and subsequent flow cytometry. These data show that induced expression of IGFBP-3 resulted in an arrest of the cell cycle in G1 phase.

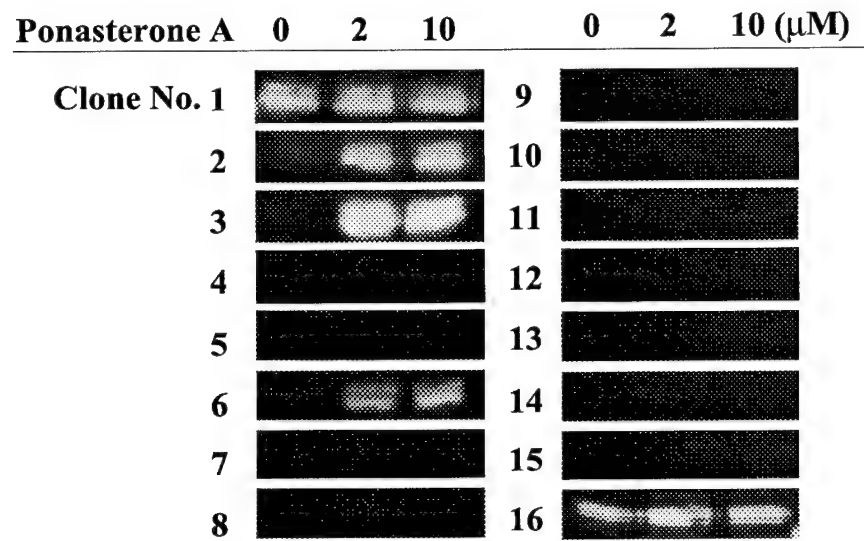
**Fig. 4.** Induced IGFBP-3 expression causes a reduction in Cyclin D1 at mRNA and protein levels. A) Northern blot analysis of a time course of cyclin D1 and IGFBP-3 expression in induced and uninduced cells. With the induction of IGFBP-3, expression of the 4.5 kb cyclin D1 mRNA species is decreased. Expression of the 1.5 kb species is not affected. B-actin was used as a control. B) Western blot analysis of Cyclin D1 protein in the MCF-7:IGFBP-3 #3 and MCF-7:EcR cells after treatment with increasing concentrations of ponasterone A for 72 h. Induction of IGFBP-3 results in a significant decrease in the level of Cyclin D1. C) Co-treatment with Y60L-IGF-I reverses the decreased level of cyclin D1 showed in IGFBP-3-induced cells, demonstrating specificity of IGFBP-3.

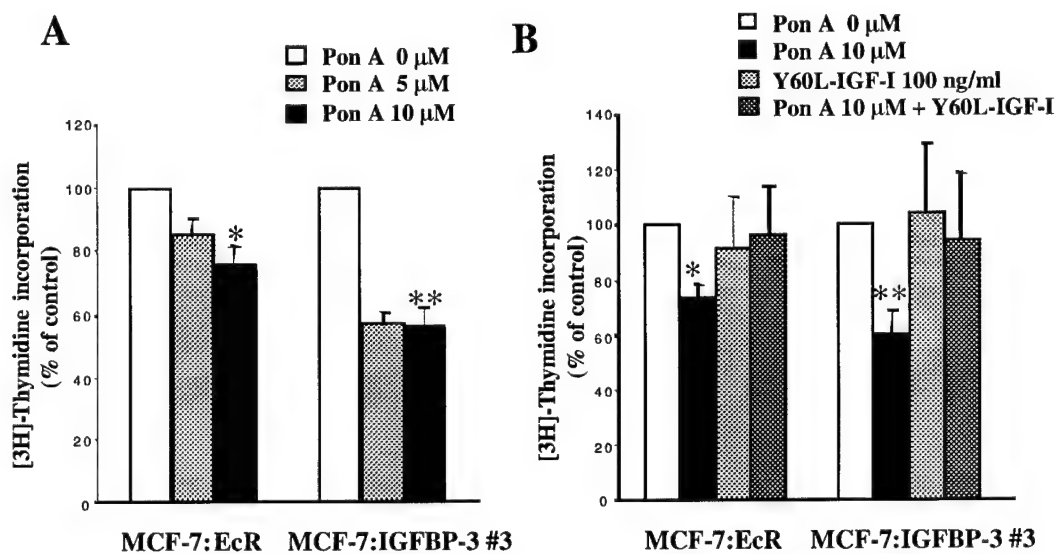
**Fig 5.** Cell cycle proteins affected by induction of IGFBP-3 expression. A) Western blot analysis of various cell cycle-related proteins in the MCF-7:IGFBP-3 #3 cells cultured in the presence or absence of ponasterone A at indicated time. The expression of cyclin D1, cdk4, total Rb, and phospho-Rb starts to decline from day 1 in the IGFBP-3-induced cells, presenting a possible direct mechanism for IGFBP-3-induced cell cycle arrest. A decrease of cyclin A expression is evident after day 3. B) Immunofluorescent staining of cells showing the decrease in Cyclin D1 and phosphorylated Rb detectable levels with the induction of IGFBP-3.

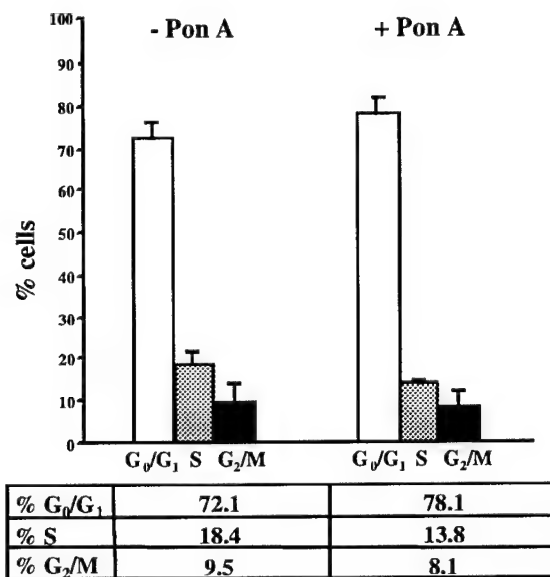
Fig. 6. IGFBP-3 induction causes a decrease in active MAPK. A) Western blot analysis of p44/42 mitogen-activated protein kinase (MAPK) and phosphorylated p44/42 MAPK in the MCF-7:IGFBP-3 #3 cells cultured the presence or absence of ponasterone A at indicated time. The phosphorylation of MAPKs declines with induction of IGFBP-3. B) Immunofluorescent staining of phospho-p44/42 MAPK in control uninduced and IGFBP-3-induced cells. A decrease in detectable levels of phospho-MAPK is evident, as well as perturbed subcellular localization.

Fig. 7. IGFBP-3 antagonizes Ras-induced MAPK signaling. MCF-7:IGFBP-3 #3 cells were transfected with a constitutively active Ras (RasV12) construct, which increased A) DNA synthesis and B) phosphorylation of p44/42 MAPK. Induction of IGFBP-3 expression abrogated both of these RasV12-induced effects.

Fig. 8. Induction of apoptosis in the MCF-7:IGFBP-3 #3 cells. A) Asynchronous MCF-7:IGFBP-3 #3 cells were seeded with or without ponasterone A for 72 h. Cells were incubated with Annexin V, then binding of Annexin V was determined by flow cytometry. IGFBP-3-induced cells showed significantly increased binding of Annexin V, an indicator of cells undergoing apoptosis. B) Asynchronous MCF-7:IGFBP-3 #3 cells were cultured with or without ponasterone A, and cell lysates were assayed for caspase activity. Induction of IGFBP-3 caused a dose-dependent increase in caspase activity compared to control uninduced levels. C) Detection of PARP cleavage to the p85 protein species as detected by western immunoblot. An increase in the p85 species was seen in lysates from IGFBP-3-induced cells compared to uninduced controls. \* = p<0.05.

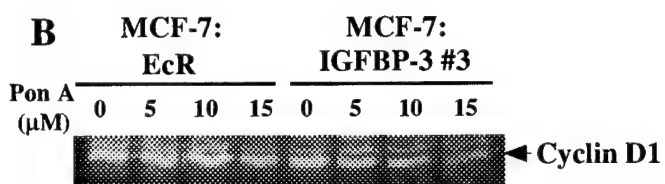
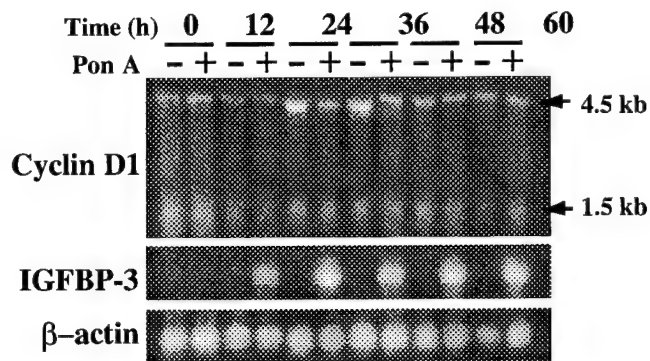




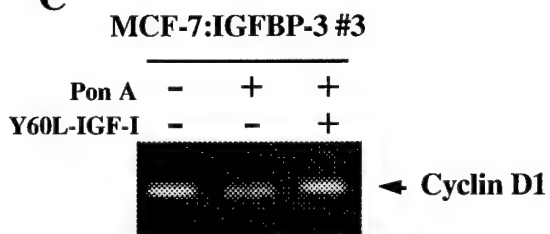


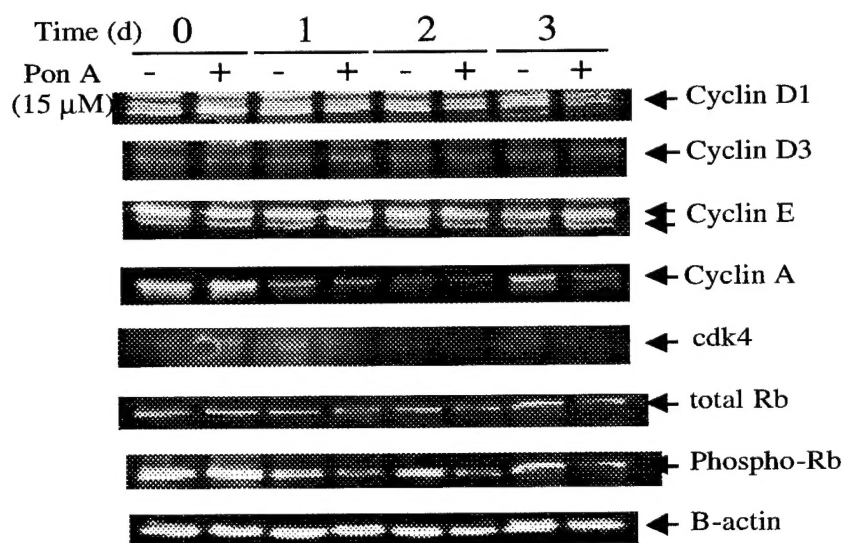
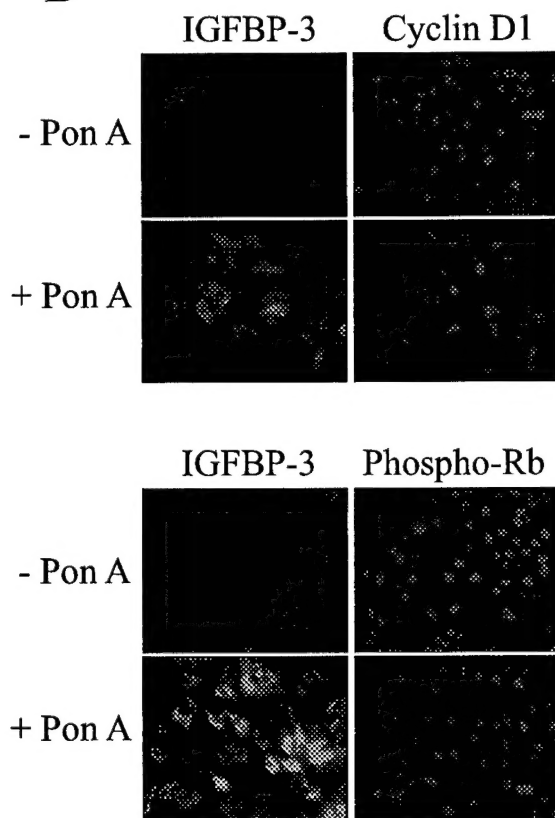
MCF-7: IGFBP-3 #3

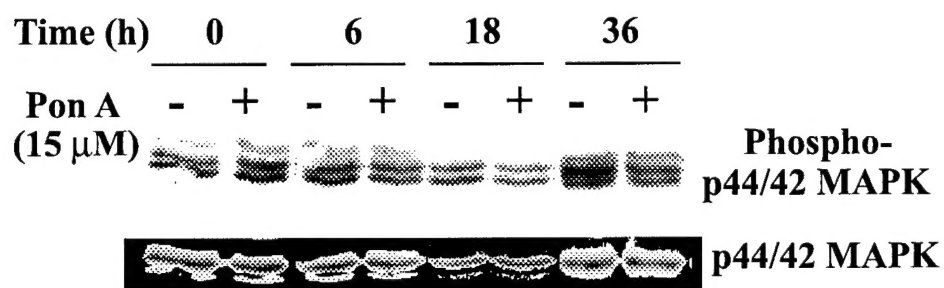
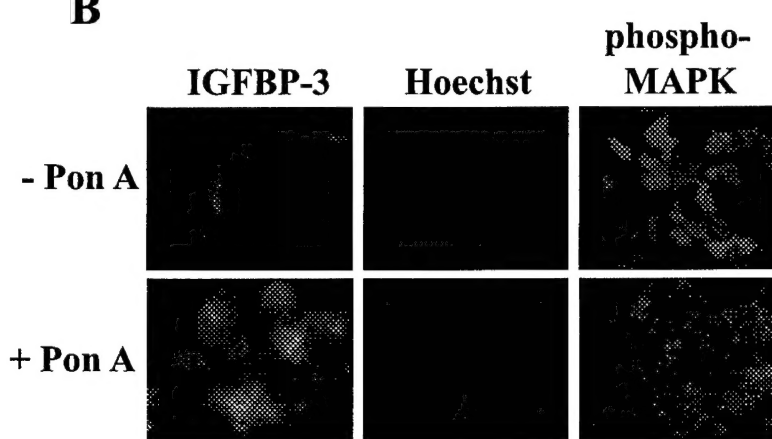
**A**

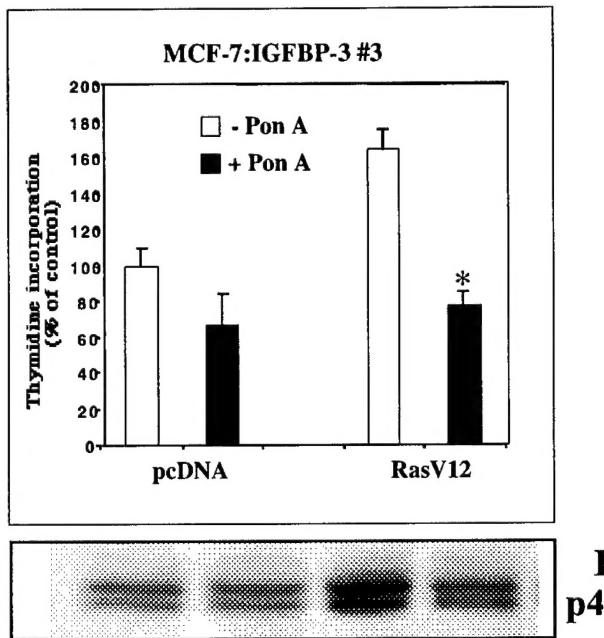


**C**

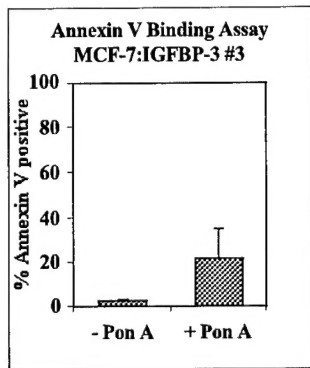
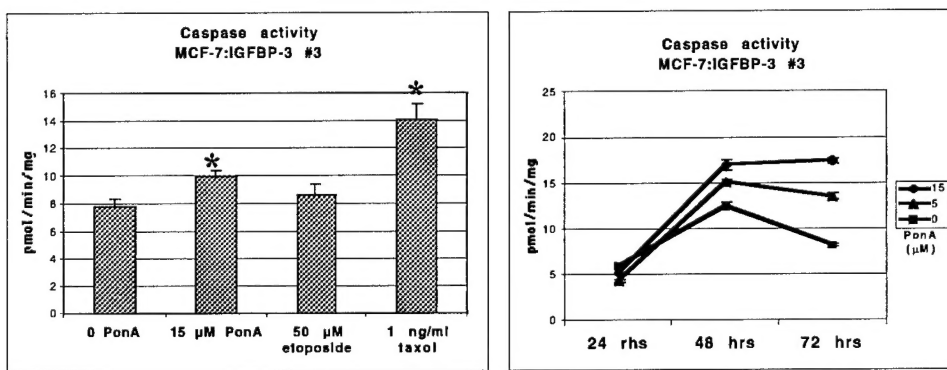


**A****B**

**A****B**



**Phospho-p44/42 MAPK**

**A****B****C**

Pon A:

- +

full length PARP

p85

